Fundamentals of Vehicle Dynamics

Thomas D. Gillespie

Published by:
Society of Automotive Engineers, Inc.
400 Commonwealth Drive
Warrendale, PA 15096-0001

TABLE OF CONTENTS

LIST OF SYMBOLS

a	Tire cornering stiffness parameter
b	Tire cornering stiffness parameter
A	Frontal area of a vehicle
A_f	Lateral force compliance steer coefficient on the front axle
A_r	Lateral force compliance steer coefficient on the rear axle
a_x	Acceleration in the x-direction
a_y	Acceleration in the lateral direction
b	Longitudinal distance from front axle to center of gravity
c	Longitudinal distance from center of gravity to rear axle
C_α	Cornering stiffness of the tires on an axle
C_α'	Cornering stiffness of one tire
CC_α	Tire cornering coefficient
C_γ	Tire camber stiffness
C_D	Aerodynamic drag coefficient
C_h	Road surface rolling resistance coefficient
C_L	Aerodynamic lift coefficient
C_{PM}	Aerodynamic pitching moment coefficient
C_{RM}	Aerodynamic rolling moment coefficient
C_{YM}	Aerodynamic yawing moment coefficient
C_s	Suspension damping coefficient
C_S	Aerodynamic side force coefficient
CP	Center of pressure location of aerodynamic side force
d	Lateral distance between steering axis and center of tire contact at the ground
d_h	Distance from axle to the hitch point
d_{ns}	Distance from center of mass to the neutral steer point
D	Tire diameter
DI	Dynamic index
D_x	Linear deceleration
D_A	Aerodynamic drag force
e	Height of the pivot for an "equivalent torque arm"
	Drum brake geometry factor
$E[y^2]$	Mean square vibration response
f	Longitudinal length for an "equivalent torque arm"
f_a	Wheel hop resonant frequency (vertical)

f_n	Undamped natural frequency of a suspension system (Hz)
f_r	Rolling resistance coefficient
F_b	Braking force
	Vertical disturbance force on the sprung mass
F_i	Imbalance force in a tire
F_x	Force in the x-direction (tractive force)
F_{xm}	Maximum brake force on an axle
F_{xt}	Total force in the x-direction
F_y	Force in the y-direction (lateral force)
	Lateral force on an axle
F_y'	Lateral force on one tire
F_z	Force in the z-direction (vertical force)
F_{zi}	Vertical force on inside tire in a turn
F_{zo}	Vertical force on outside tire in a turn
F_w	Tire/wheel nonuniformity force on the unsprung mass
g	Acceleration of gravity (32.2 ft/sec^2, 9.81 m/sec^2)
G	Brake gain
G_o	Road roughness magnitude parameter
G_z	Power spectral density amplitude of road roughness
G_{zs}	Power spectral density amplitude of sprung mass acceleration
h	Center of gravity height
h_a	Height of the aerodynamic drag force
h_h	Hitch height
h_l	Height of the sprung mass center of gravity above the roll axis
h_r	Height of suspension roll center
h_t	Tire section height
HP	Engine or brake horsepower
HP_A	Aerodynamic horsepower
HP_R	Rolling resistance horsepower
HP_{RL}	Road load horsepower
H_v	Response gain function
I_d	Moment of inertia of the driveshaft
I_e	Moment of inertia of the engine
I_t	Moment of inertia of the transmission
I_w	Moment of inertia of the wheels
I_{xx}	Moment of inertia about the x-axis

I_{yy}	Moment of inertia about the y-axis
I_{zz}	Moment of inertia about the z-axis
k	Radius of gyration
K	Understeer gradient
K_{at}	Understeer gradient due to aligning torque
K_{llt}	Understeer gradient due to lateral load transfer on the axles
K_{lfcs}	Understeer gradient due to lateral force compliance steer
K_s	Vertical stiffness of a suspension
K_{ss}	Steering system stiffness
K_{strg}	Understeer gradient due to the steering system
K_t	Vertical stiffness of a tire
K_ϕ	Suspension roll stiffness
L	Wheelbase
L_A	Aerodynamic lift force
m	Drum brake geometry parameter
M	Mass of the vehicle
M_{AT}	Moment around the steer axis due to tire aligning torques
M_L	Moment around the steer axis due to tire lateral forces
M_r	Equivalent mass of the rotating components
M_{SA}	Moment around the steer axis due to front-wheel-drive forces and torques
M_T	Moment around the steer axis due to tire tractive forces
M_V	Moment around the steer axis due to tire vertical forces
M_ϕ	Rolling moment
n	Drum brake geometry parameter
N	Normal force
N_t	Numerical ratio of the transmission
N_f	Numerical ratio of the final drive
N_{tf}	Numerical ratio of the combined transmission and final drive
NSP	Neutral steer point
p	Pneumatic trail
P_a	Brake application pressure/effort
P_{atm}	Atmospheric pressure
P_f	Front brake application pressure
P_r	Rear brake application pressure
P_s	Static pressure
P_t	Total pressure

PM	Aerodynamic pitching moment
p	Roll velocity about the x-axis of the vehicle
q	Pitch velocity about the y-axis of the vehicle
q	Dynamic pressure
r	Yaw velocity about the z-axis of the vehicle
r	Rolling radius of the tires
r_k	Ratio of tire to suspension stiffness
R	Radius of turn
R_h	Hitch force
R_g	Grade force
R_x	Rolling resistance force
R_{RL}	Road load
RM	Aerodynamic rolling moment
RR	Ride rate of a tire/suspension system
R_ϕ	Roll rate of the sprung mass
s	Lateral separation between suspension springs
S_A	Aerodynamic side force
S_o	Spectral density of white-noise
SD	Stopping distance
t	Tread
t_s	Length of time of a brake application
T_a	Torque in the axle
T_b	Brake torque
T_c	Torque at the clutch
T_d	Torque in the driveshaft
T_e	Torque of the engine
T_{sf}	Roll torque in a front suspension
T_{sr}	Roll torque in a rear suspension
T_{amb}	Ambient temperature
T_x	Torque about the x-axis
V	Forward velocity
V_w	Ambient wind velocity
V_f	Final velocity resulting from a brake application
V_o	Initial velocity in a brake application
w	Tire section width
W	Weight of the vehicle

W_a	Axle weight
W_d	Dynamic load transfer
W_f	Dynamic weight on the front axle
W_r	Dynamic weight on the rear axle
W_{rr}	Dynamic weight on the right rear wheel
W_{fs}	Static weight on the front axle
W_{rs}	Static weight on the rear axle
W_y	Lateral weight transfer on an axle
x	Forward direction on the longitudinal axis of the vehicle
y	Lateral direction out the right side of the vehicle
YM	Aerodynamic yawing moment
z	Vertical direction with respect to the plane of the vehicle
X	Forward direction of travel
Y	Lateral direction of travel
Z	Vertical direction of travel
	Vertical displacement of the sprung mass
Z_r	Road profile elevation
Z_u	Vertical displacement of the unsprung mass
α	Tire slip angle
	Coefficient in the pitch plane equations
α_{cw}	Aerodynamic wind angle
α_d	Rotational acceleration of the driveshaft
α_e	Rotational acceleration of the engine
α_w	Rotational acceleration of the wheels
α_x	Rotational acceleration about the x-axis
β	Sideslip angle
	Rotation angle of a U-joint
	Coefficient in the pitch plane equations
γ	Camber angle
	Coefficient in the pitch plane equations
γ_g	Wheel camber with respect to the ground
γ_b	Wheel camber with respect to the vehicle body
δ	Steer angle
δ_c	Compliance steer
δ_i	Steer angle of the inside wheel in a turn

δ_o	Steer angle of the outside wheel in a turn
Δ	Off-tracking distance in a turn
ε	Roll steer coefficient
	Inclination of the roll axis
ζ	Moment arm related to tire force yaw damping
	Half-shaft angle on a front-wheel drive
ζ_s	Damping ratio of the suspension
η_b	Braking efficiency
η_t	Efficiency of the transmission
η_f	Efficiency of the final drive
η_{tf}	Combined efficiency of the transmission and final drive
θ	Pitch angle
	Angle of a U-joint
θ_p	Body pitch due to acceleration squat or brake dive
Θ	Grade angle
λ	Lateral inclination angle of the steer axis (kingpin inclination angle)
μ	Coefficient of friction
μ_p	Peak coefficient of friction
μ_s	Sliding coefficient of friction
ν	Wavenumber of road roughness spectrum
ξ	Fraction of the drive force developed on the front axle of a 4WD
	Fraction of the brake force developed on the front axle
	Rear steer proportioning factor on a 4WS vehicle
ρ	Density of air
υ	Caster angle of the steer axis
ϕ	Roll angle
φ	Road cross-slope angle
χ	Ratio of unsprung to sprung mass
ψ	Heading angle
	Yaw angle
ω	Rotational speed
ω_d	Damped natural frequency of a suspension system (radians/second)
	Rotational speed of the driveshaft
ω_e	Rotational speed of the engine
ω_i	Rotational speed at the input of a U-joint
ω_n	Undamped natural frequency of a suspension system (radians/second)

ω_o	Rotational speed at the output of a U-joint
ω_u	Natural frequency of the unsprung mass
ω_w	Rotational speed of the wheels

CHAPTER 1
INTRODUCTION

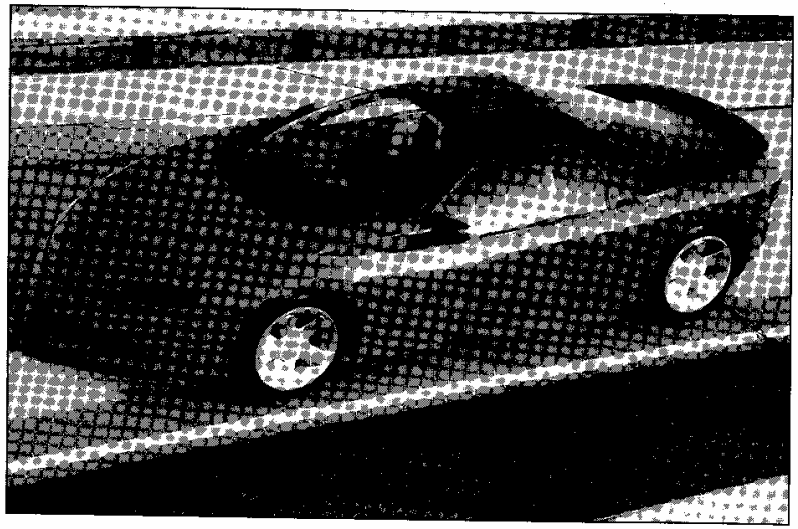

The next-generation Camaro. (Photo courtesy of Chevrolet Motor Division.)

DAWN OF THE MOTOR VEHICLE AGE

The dawn of the motor vehicle age occurred around 1769 when the French military engineer, Nicholas Joseph Cugnot (1725-1804), built a three-wheeled, steam-driven vehicle for the purpose of pulling artillery pieces [1]. Within a few years an improved model was built, only to cause the first automotive accident when it ran into a wall! This was followed by a steam-powered vehicle built in 1784 by the Scottish engineer, James Watt (1736-1819), which proved unworkable. By 1802, Richard Trevithick (1771-1833), an Englishman, developed a steam coach that traveled from Cornwall to London. The coach met its demise by burning one night after Trevithick forgot to extinguish the boiler fire. Nevertheless, the steam coach business thrived in England until about 1865 when competition from the railroads and strict antispeed laws brought it to an end [2].

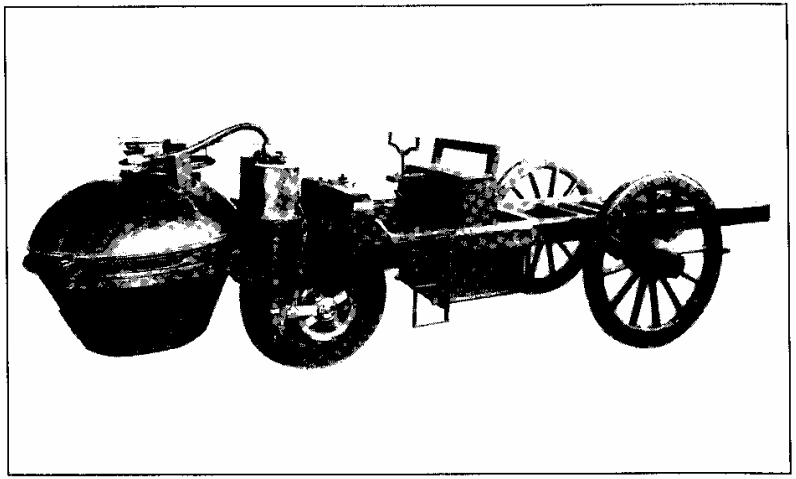

Fig. 1.1 First motor vehicle, circa 1769, built by Cugnot. (Photo courtesy of Smithsonian Institution.)

The first practical automobiles powered by gasoline engines arrived in 1886 with the credit generally going to Karl Benz (1844-1929) and Gottlieb Daimler (1834-1900) working independently. Over the next decade, automotive vehicles were developed by many other pioneers with familiar names such as Rene Panhard, Emile Levassor, Armand Peugeot, Frank and Charles Duryea, Henry Ford, and Ransom Olds. By 1908 the automotive industry was well established in the United States with Henry Ford manufacturing the Model T and the General Motors Corporation being founded. In Europe the familiar companies like Daimler, Opel, Renault, Benz, and Peugeot were becoming recognized as automotive manufacturers. By 1909, over 600 makes of American cars had been identified [3].

In the early decades of the 1900s, most of the engineering energy of the automotive industry went into invention and design that would yield faster, more comfortable, and more reliable vehicles. The speed capability of motor vehicles climbed quickly in the embryonic industry as illustrated by the top speeds of some typical production cars, as shown in Figure 1.2.

In general, motor vehicles achieved high speed capability well before good paved roads existed on which to use it. With higher speeds the dynamics of the vehicles, particularly turning and braking, assumed greater importance as an engineering concern. The status of automotive engineering during this period was characterized in the reminiscences of Maurice Olley [4] as follows:

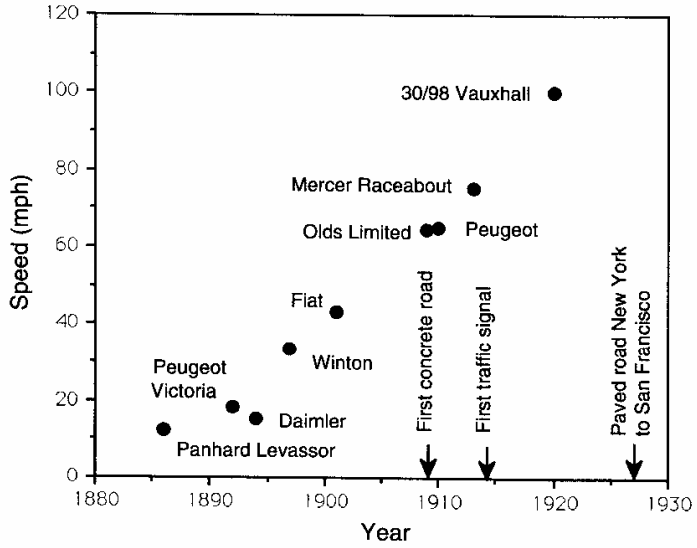

Fig. 1.2 Travel speeds of production automobiles.

"There had been sporadic attempts to make the vehicle ride decently, but little had been done. The rear passengers still functioned as ballast, stuck out behind the rear wheels. Steering was frequently unstable and the front axle with front brakes made shimmy almost inevitable. The engineers had made all the parts function excellently, but when put together the whole was seldom satisfactory."

One of the first engineers to write on automotive dynamics was Frederick William Lanchester (1868-1946). (In a 1908 paper [5] he observed that a car with tiller steering "oversteers" if the centrifugal force on the driver's hands pushes toward greater steer angle [6].) Steering shimmy problems were prevalent at that time as well [7, 8]. But, as described by Segel [6], the understanding of both turning behavior and the shimmy problems was hampered by a lack of knowledge about tire mechanics in these early years.

In 1931, a test device—a tire dynamometer—was built which could measure the necessary mechanical properties of the pneumatic tire for the understandings to be developed [9]. Only then could engineers like Lanchester [10], Olley [11], Rieckert and Schunk [12], Rocard [13], Segel [14] and others develop mechanistic explanations of the turning behavior of automobiles which lays the groundwork for much of our understanding today.

The industry has now completed its first century. Engineers have achieved dramatic advancements in the technologies employed in automobiles from the Model T to the Taurus (Figure 1.3). More than ever, dynamics plays an important role in vehicle design and development. A number of textbooks have been written to help the engineer in this discipline [15 - 24], but there remains a need for books that lay out the fundamental aspects of vehicle dynamics. This book attempts to fill that need.

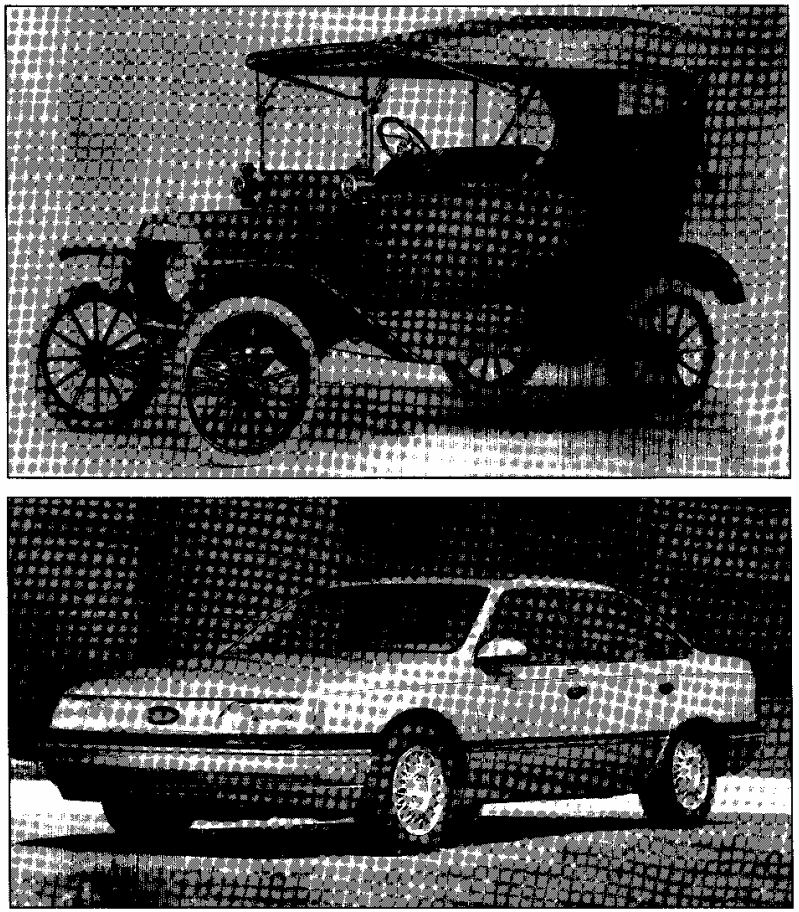

Fig. 1.3 Eighty years of progress from the Model T to the Taurus. (Photos courtesy of Henry Ford Museum and Ford Motor Company.)

INTRODUCTION TO VEHICLE DYNAMICS

It has often been said that the primary forces by which a high-speed motor vehicle is controlled are developed in four patches—each the size of a man's hand—where the tires contact the road. This is indeed the case. A knowledge of the forces and moments generated by pneumatic (rubber) tires at the ground is essential to understanding highway vehicle dynamics. Vehicle dynamics in its broadest sense encompasses all forms of conveyance—ships, airplanes, railroad trains, track-laying vehicles, as well as rubber-tired vehicles. The principles involved in the dynamics of these many types of vehicles are diverse and extensive. Therefore, this book focuses only on rubber-tired vehicles. Most of the discussion and examples will concentrate on the automobile, although the principles are directly applicable to trucks and buses, large and small. Where warranted, trucks will be discussed separately when the functional design or performance qualities distinguish them from the automobile.

Inasmuch as the performance of a vehicle—the motions accomplished in accelerating, braking, cornering and ride—is a response to forces imposed, much of the study of vehicle dynamics must involve the study of how and why the forces are produced. The dominant forces acting on a vehicle to control performance are developed by the tire against the road. Thus it becomes necessary to develop an intimate understanding of the behavior of tires, characterized by the forces and moments generated over the broad range of conditions over which they operate. Studying tire performance without a thorough understanding of its significance to the vehicle is unsatisfying, as is the inverse. Therefore, the relevant properties of tires are introduced at appropriate points in the early chapters of the text, while the reader is referred to Chapter 10 for a more comprehensive discussion of tire properties.

At the outset it is worth noting that the term "handling" is often used interchangeably with cornering, turning, or directional response, but there are nuances of difference between these terms. Cornering, turning, and directional response refer to objective properties of the vehicle when changing direction and sustaining lateral acceleration in the process. For example, cornering ability may be quantified by the level of lateral acceleration that can be sustained in a stable condition, or directional response may be quantified by the time required for lateral acceleration to develop following a steering input. Handling, on the other hand, adds to this the vehicle qualities that feed back to the driver affecting the ease of the driving task or affecting the driver's ability to maintain control. Handling implies, then, not only the vehicle's explicit capabilities, but its contributions as well to the system performance of the driver/vehicle combination. Throughout the book the various terms will be used in a manner most appropriate to the discussion at hand.

Understanding vehicle dynamics can be accomplished at two levels—the empirical and the analytical. The empirical understanding derives from trial and error by which one learns which factors influence vehicle performance, in which way, and under what conditions. The empirical method, however, can often lead to failure. Without a mechanistic understanding of how changes in vehicle design or properties affect performance, extrapolating past experience to new conditions may involve unknown factors which may produce a new result, defying the prevailing rules of thumb. For this reason (and because they are methodical by nature), engineers favor the analytical approach. The analytical approach attempts to describe the mechanics of interest based on the known laws of physics so that an analytical model can be established. In the simpler cases these models can be represented by algebraic or differential equations that relate forces or motions of interest to control inputs and vehicle or tire properties. These equations then allow one to evaluate the role of each vehicle property in the phenomenon of interest. The existence of the model thereby provides a means to identify the important factors, the way in which they operate, and under what conditions. The model provides a predictive capability as well, so that changes necessary to reach a given performance goal can be identified.

It might be noted at this point that analytical methods also are not foolproof because they usually only approximate reality. As many have experienced, the assumptions that must be made to obtain manageable models may often prove fatal to an application of the analysis, and on occasion engineers have been found to be wrong. Therefore, it is very important for the engineer to understand the assumptions that have been made in modeling any aspect of dynamics to avoid these errors.

In the past, many of the shortcomings of analytical methods were a consequence of the mathematical limitations in solving problems. Before the advent of computers, analysis was only considered successful if the "problem" could be reduced to a closed form solution. That is, only if the mathematical expression could be manipulated to a form which allowed the analyst to extract relationships between the variables of interest. To a large extent this limited the functionality of the analytical approach to solution of problems in vehicle dynamics. The existence of large numbers of components, systems, subsystems, and nonlinearities in vehicles made comprehensive modeling virtually impossible, and the only utility obtained came from rather simplistic models of certain mechanical systems. Though useful, the simplicity of the models often constituted deficiencies that handicapped the engineering approach in vehicle development.

Today with the computational power available in desktop and mainframe computers, a major shortcoming of the analytical method has been overcome. It is now possible to assemble models (equations) for the behavior of individual components of a vehicle that can be integrated into comprehensive models of the overall vehicle, allowing simulation and evaluation of its behavior before being rendered in hardware. Such models can calculate performance that could not be solved for in the past. In cases where the engineer is uncertain of the importance of specific properties, those properties can be included in the model and their importance assessed by evaluating their influence on simulated behavior. This provides the engineer with a powerful new tool as a means to test our understanding of a complex system and investigate means of improving performance. In the end we are forced to confront all the variables that may influence the performance of interest, and recognize everything that is important.

FUNDAMENTAL APPROACH TO MODELING

The subject of "vehicle dynamics" is concerned with the movements of vehicles—automobiles, trucks, buses, and special-purpose vehicles—on a road surface. The movements of interest are acceleration and braking, ride, and turning. Dynamic behavior is determined by the forces imposed on the vehicle from the tires, gravity, and aerodynamics. The vehicle and its components are studied to determine what forces will be produced by each of these sources at a particular maneuver and trim condition, and how the vehicle will respond to these forces. For that purpose it is essential to establish a rigorous approach to modeling the systems and the conventions that will be used to describe motions.

Lumped Mass

A motor vehicle is made up of many components distributed within its exterior envelope. Yet, for many of the more elementary analyses applied to it, all components move together. For example, under braking, the entire vehicle slows down as a unit; thus it can be represented as one lumped mass located at its center of gravity (CG) with appropriate mass and inertia properties. For acceleration, braking, and most turning analyses, one mass is sufficient. For ride analysis, it is often necessary to treat the wheels as separate lumped masses. In that case the lumped mass representing the body is the "sprung mass," and the wheels are denoted as "unsprung masses."

For single mass representation, the vehicle is treated as a mass concentrated at its center of gravity (CG) as shown in Figure 1.4. The point mass at

the CG, with appropriate rotational moments of inertia, is dynamically equivalent to the vehicle itself for all motions in which it is reasonable to assume the vehicle to be rigid.

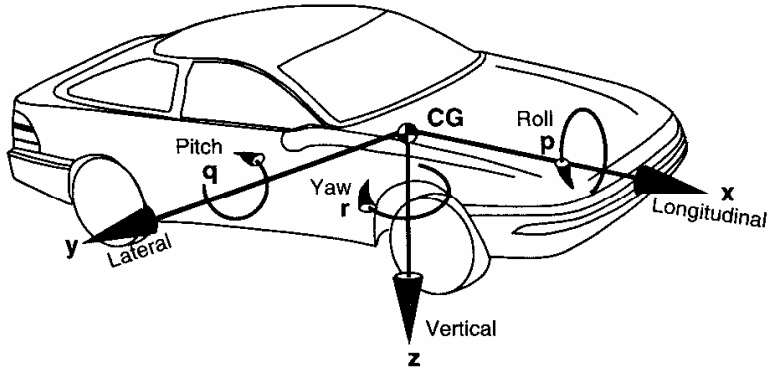

Fig. 1.4 SAE Vehicle Axis System.

Vehicle Fixed Coordinate System

On-board, the vehicle motions are defined with reference to a right-hand orthogonal coordinate system (the vehicle fixed coordinate system) which originates at the CG and travels with the vehicle. By SAE convention [25] the coordinates are:

- x - Forward and on the longitudinal plane of symmetry
- y - Lateral out the right side of the vehicle
- z - Downward with respect to the vehicle
- **p** - Roll velocity about the x axis
- **q** - Pitch velocity about the y axis
- **r** - Yaw velocity about the z axis

Motion Variables

Vehicle motion is usually described by the velocities (forward, lateral, vertical, roll, pitch and yaw) with respect to the vehicle fixed coordinate system, where the velocities are referenced to the earth fixed coordinate system.

Earth Fixed Coordinate System

Vehicle attitude and trajectory through the course of a maneuver are defined with respect to a right-hand orthogonal axis system fixed on the earth. It is normally selected to coincide with the vehicle fixed coordinate system at the point where the maneuver is started. The coordinates (see Figure 1.5) are:

X - Forward travel

Y - Travel to the right

Z - Vertical travel (positive downward)

ψ - Heading angle (angle between x and X in the ground plane)

ν - Course angle (angle between the vehicle's velocity vector and X axis)

β - Sideslip angle (angle between x axis and the vehicle velocity vector)

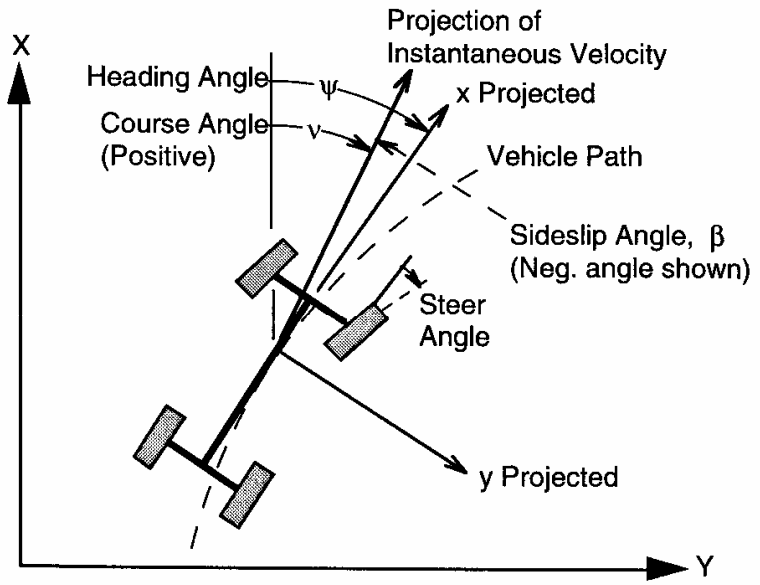

Fig. 1.5 Vehicle in an Earth Fixed Coordinate System.

Euler Angles

The relationship of the vehicle fixed coordinate system to the earth fixed coordinate system is defined by Euler angles. Euler angles are determined by a sequence of three angular rotations. Beginning at the earth fixed system, the axis system is first rotated in yaw (around the z axis), then in pitch (around the y axis), and then in roll (around the x axis) to line up with the vehicle fixed coordinate system. The three angles obtained are the Euler angles. It is necessary to adhere strictly to the defined sequence of rotations, because the resultant attitude will vary with the order of rotations.

Forces

Forces and moments are normally defined as they act on the vehicle. Thus a positive force in the longitudinal (x-axis) direction on the vehicle is forward. The force corresponding to the load on a tire acts in the upward direction and is therefore negative in magnitude (in the negative z-direction). Because of the inconvenience of this convention, the SAE J670e, "Vehicle Dynamics Terminology," gives the name Normal Force as that acting downward, and Vertical Force as the negative of the Normal Force. (See Appendix A.) Thus the Vertical Force is the equivalent of tire load with a positive convention in the upward direction. In other countries, different conventions may be used.

Given these definitions of coordinate systems and forces, it is now possible to begin formulating equations by which to analyze and describe the behavior of a vehicle.

Newton's Second Law

The fundamental law from which most vehicle dynamics analyses begin is the second law formulated by Sir Isaac Newton (1642-1727). The law applies to both translational and rotational systems [26].

Translational systems - The sum of the external forces acting on a body in a given direction is equal to the product of its mass and the acceleration in that direction (assuming the mass is fixed).

$$\Sigma F_X = M \cdot a_X \tag{1-1}$$

where:

F_X = Forces in the x-direction
M = Mass of the body
a_X = Acceleration in the x-direction

Rotational Systems - The sum of the torques acting on a body about a given axis is equal to the product of its rotational moment of inertia and the rotational acceleration about that axis.

$$\Sigma T_x = I_{xx} \cdot \alpha_x \qquad (1\text{-}2)$$

where:

T_x = Torques about the x-axis
I_{xx} = Moment of inertia about the x-axis
α_x = Acceleration about the x-axis

Newton's Second Law (NSL) is applied by visualizing a boundary around the body of interest. The appropriate forces and/or moments are substituted at each point of contact with the outside world, along with any gravitational forces. This forms a free-body diagram. A NSL equation may then be written for each of the three independent directions (normally the vehicle fixed axes).

DYNAMIC AXLE LOADS

Determining the axle loadings on a vehicle under arbitrary conditions is a first simple application of Newton's Second Law. It is an important first step in analysis of acceleration and braking performance because the axle loads determine the tractive effort obtainable at each axle, affecting the acceleration, gradeability, maximum speed, and drawbar effort.

Consider the vehicle shown in Figure 1.6, in which most of the significant forces on the vehicle are shown.

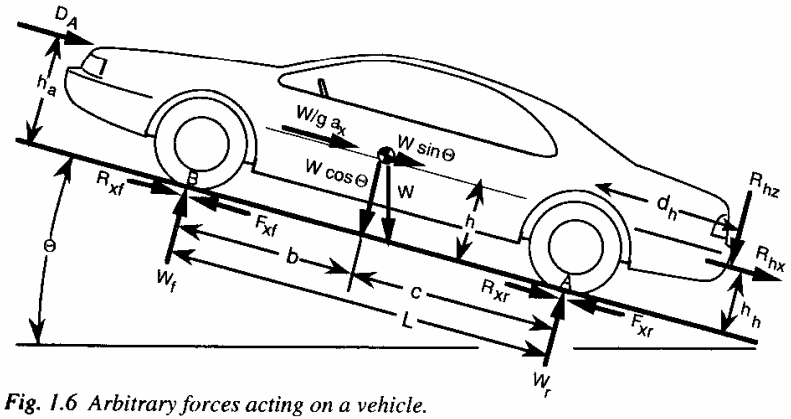

Fig. 1.6 Arbitrary forces acting on a vehicle.

- W is the weight of the vehicle acting at its CG with a magnitude equal to its mass times the acceleration of gravity. On a grade it may have two components, a cosine component which is perpendicular to the road surface and a sine component parallel to the road.
- If the vehicle is accelerating along the road, it is convenient to represent the effect by an equivalent inertial force known as a "d'Alembert force" (Jean le Rond d'Alembert, 1717-1783) denoted by $W/g \cdot a_x$ acting at the center of gravity opposite to the direction of the acceleration [26].
- The tires will experience a force normal to the road, denoted by W_f and W_r, representing the dynamic weights carried on the front and rear wheels.
- Tractive forces, F_{xf} and F_{xr}, or rolling resistance forces, R_{xf} and R_{xr}, may act in the ground plane in the tire contact patch.
- D_A is the aerodynamic force acting on the body of the vehicle. It may be represented as acting at a point above the ground indicated by the height, h_a, or by a longitudinal force of the same magnitude in the ground plane with an associated moment (the aerodynamic pitching moment) equivalent to D_A times h_a.
- R_{hz} and R_{hx} are vertical and longitudinal forces acting at the hitch point when the vehicle is towing a trailer.

The loads carried on each axle will consist of a static component, plus load transferred from front to rear (or vice versa) due to the other forces acting on the vehicle. The load on the front axle can be found by summing torques about the point "A" under the rear tires. Presuming that the vehicle is not accelerating in pitch, the sum of the torques at point A must be zero.

By the SAE convention, a clockwise torque about A is positive. Then:

$$W_f L + D_A h_a + \frac{W}{g} a_x h + R_{hx} h_h + R_{hz} d_h + W h \sin\Theta - W c \cos\Theta = 0 \qquad (1\text{-}3)$$

Note that an uphill attitude corresponds to a positive angle, Θ, such that the sine term is positive. A downhill attitude produces a negative value for this term.

From Eq. (1-3) we can solve for W_f and from a similar equation about point B we can solve for W_r. The axle load expressions then become:

$$W_f = (W\,c\cos\Theta - R_{hx}\,h_h - R_{hz}\,d_h - \frac{W}{g}\,a_x\,h - D_A\,h_a - W\,h\sin\Theta)/L \tag{1-4}$$

$$W_r = (W\,b\cos\Theta + R_{hx}\,h_h + R_{hz}\,(d_h + L) + \frac{W}{g}\,a_x\,h + D_a\,h_a + W\,h\sin\Theta)/L \tag{1-5}$$

Static Loads on Level Ground

When the vehicle sits statically on level ground, the load equations simplify considerably. The sine is zero and the cosine is one, and the variables R_{hx}, R_{hz}, a_x, and D_A are zero. Thus:

$$W_{fs} = W\frac{c}{L} \tag{1-6}$$

$$W_{rs} = W\frac{b}{L} \tag{1-7}$$

Low-Speed Acceleration

When the vehicle is accelerating on level ground at a low speed, such that D_A is zero (and presuming no trailer hitch forces), the loads on the axles are:

$$W_f = W\left(\frac{c}{L} - \frac{a_x}{g}\frac{h}{L}\right) = W_{fs} - W\frac{a_x}{g}\frac{h}{L} \tag{1-8}$$

$$W_r = W\left(\frac{b}{L} + \frac{a_x}{g}\frac{h}{L}\right) = W_{rs} + W\frac{a_x}{g}\frac{h}{L} \tag{1-9}$$

Thus when the vehicle accelerates, load is transferred from the front axle to the rear axle in proportion to the acceleration (normalized by the gravitational acceleration) and the ratio of the CG height to the wheelbase.

Loads on Grades

The influence of grade on axle loads is also worth considering. Grade is defined as the "rise" over the "run." That ratio is the tangent of the grade angle, Θ. The common grades on interstate highways are limited to 4 percent wherever possible. On primary and secondary roads they occasionally reach 10 to 12 percent. The cosines of angles this small are very close to one, and the sine is very close to the angle itself. That is:

$$\cos\Theta = 0.99^{+} \cong 1$$

$$\sin\Theta \cong \Theta$$

Thus the axle loads as influenced by grades will be:

$$W_f = W\left(\frac{c}{L} - \frac{h}{L}\Theta\right) = W_{fs} - W\frac{h}{L}\Theta \tag{1-10}$$

$$W_r = W\left(\frac{b}{L} + \frac{h}{L}\Theta\right) = W_{rs} + W\frac{h}{L}\Theta \tag{1-11}$$

where a positive grade causes load to be transferred from the front to the rear axle.

EXAMPLE PROBLEMS

1) The curb weights of a Continental 4-door sedan without passengers or cargo are 2313 lb on the front axle and 1322 lb on the rear. The wheelbase, L, is 109 inches. Determine the fore/aft position of the center of gravity for the vehicle.

Solution:

The fore/aft position of the CG is defined by either parameter c or b in Eqs. (1-6) or (1-7), which apply to a vehicle sitting at rest on level ground. Using Eq. (1-7) we can solve for b:

$$b = L\frac{W_{rs}}{W} = 109"\ \frac{1322\text{ lb}}{(2313 + 1322)\text{ lb}} = 39.64"$$

i.e., the CG of the vehicle is 39.64 inches aft of the front axle.

2) A Taurus GL sedan with 3.0L engine accelerates from a standing start up a 6 percent grade at an acceleration of 6 ft/sec^2. Find the load distribution on the axles at this condition.

Solution:

Assume that aerodynamic forces are negligible since the vehicle starts from zero speed, and there are no trailer hitch forces. Equations (1-4) and (1-5) are the fundamental equations from which to start, but to use them the values for the parameters b and c must be determined. To obtain these check the MVMA (Motor Vehicle Manufacturers Association) specification sheets for the Taurus GL sedan for relevant data. The curb weights are 1949 lb on the

front axle and 1097 lb on the rear; the wheelbase is 106 inches; and front passenger's weight is distributed 49 percent on the front axle and 51 percent on the rear. Assuming a 200 lb driver this gives weights as follows:

$$W_{fs} = 2047 \text{ lb} \quad W_{rs} = 1199 \text{ lb} \quad W = 3246 \text{ lb}$$

Eqs. (1-6) and (1-7) are used to find that b = 39.15 inches and c = 66.85 inches. From a pocket calculator we determine that a 6 percent grade corresponds to a 3.433 degree angle (arctangent of 0.06). Lacking a source for information on CG height, h, assume it is 20 inches. Now all of the information is available to solve equation (1-4).

$$W_f = \frac{W(c \cos \Theta - h\, a_x/g - h \sin \Theta)}{L}$$

$$W_f = \frac{3246 \text{ lb } (66.85" \ 0.998 - 20" \ 6/32.2 - 20" \ 0.0599)}{106"} = 1892.2 \text{ lb}$$

Using the same approach the rear axle load is found to be 1347.3 lb. Curiously, these only add up to about 3239.5 lb, not the 3246 lb weight of the car. Why? The reason, of course, is that the vehicle is sitting on a slope. Only the cosine of the weight vector acts to produce load on the axles. Thus, the weight on the axles should only add up to 3246 lb times cos 3.433° = 3240 lb.

3) You are planning to buy a new mini-van to pull your boat trailer (see below) out to those long weekends at the lake. Although you like the new front-wheel-drive (FWD) vans available, you are not sure a FWD will be able to pull the boat up out of the water on some of the steep access ramps you must use.

a) Derive the expressions for the maximum grade it can climb without wheel slippage (traction-limited gradeability) for this vehicle combination in a front-wheel-drive (FWD), rear-wheel-drive (RWD), and four-wheel-drive (4WD) power train.

(In the analysis it is reasonable to assume the longitudinal acceleration is zero, neglect rolling resistance, assume the boat is clear of the water so that there are no bouyancy forces on it, ignore any change in hitch height as the forces are applied, and use the small angle approximations.)

b) Calculate the maximum gradeability for the three combinations on a ramp with a coefficient of friction of 0.3, given the following information on the vehicles.

Van properties:
Front axle weight = 1520 lb
Rear axle weight = 1150 lb
CG height = 24.5 inches
Hitch height = 14 inches
Hitch rear overhang = 23 inches
Wheelbase = 120 inches

Combined boat/trailer properties:
Axle weight = 1200 lb
Hitch load = 250 lb
Wheelbase = 110 inches
CG height = 35 inches

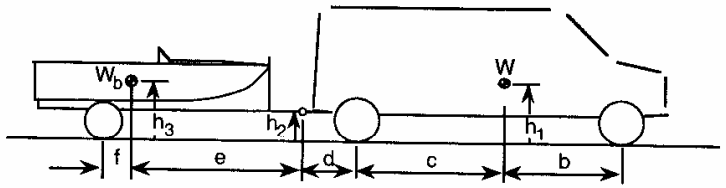

Solution:

In order to derive the equations for traction-limited gradeability, first perform a free-body analysis of the boat trailer to find the hitch forces as a function of grade.

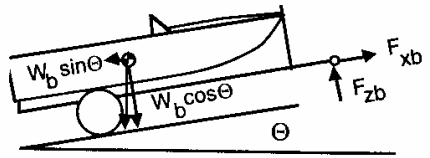

Taking moments about the point where the tire contacts the ground (counterclockwise moments are positive):

$$\Sigma T_y = 0 = W_b h_3 \sin \Theta + F_{zb} (e + f) - W_b f \cos \Theta - F_{xb} h_2 \qquad (1)$$

Also, the force balance along the longitudinal axis of the boat trailer gives:

$$\Sigma F_x = 0 = F_{xb} - W_b \sin \Theta \qquad (2)$$

Next we perform a similar analysis on the van.

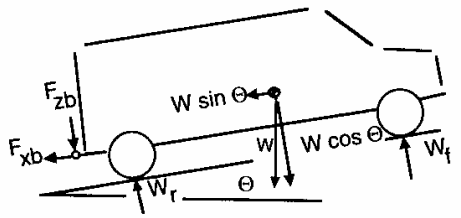

Taking moments about the rear tire contact point:

$$\Sigma T_y = 0 = W h_1 \sin\Theta - W c \cos\Theta + F_{zb} d + F_{xb} h_2 + W_f (b + c) \quad (3)$$

And for moments about the front axle:

$$\Sigma T_y = 0 = W h_1 \sin\Theta + W b \cos\Theta + F_{zb} (b + c + d) + F_{xb} h_2 - W_r (b + c) \quad (4)$$

There are four equations and four unknowns (F_{zb}, F_{xb}, W_f, W_r). We can therefore solve for any one of the unknowns desired. For the case of the FWD, the traction limit will be determined by the load on the front axle times the coefficient of friction, μ. The solution is obtained from Eq. (3), using Eqs. (1) and (2) to eliminate the hitch forces from the final equation. The tractive force will be equal to the combined weight of the van and boat times the grade angle. That is:

$$(W + W_b) \sin\Theta = F_{xf} = \mu W_f \quad (5)$$

$$= \mu \left[W \frac{c}{L} \cos\Theta - W \frac{h_1}{L} \sin\Theta - W_b \frac{h_2}{L} \sin\Theta \right.$$

$$\left. + W_b \frac{d}{L} \frac{h_3}{L_t} \sin\Theta - W_b \frac{d}{L} \frac{f}{L_t} \cos\Theta - W_b \frac{d}{L} \frac{h_2}{L_t} \sin\Theta \right]$$

The trigonometric functions in the equation make it complicated to obtain a simplified solution. Using the small angle approximations, $\sin\Theta$ can be replaced with Θ, and $\cos\Theta$ can be treated as 1. It is also convenient to define several alternate variables for use in the solution. These will be:

$L = b + c$ = Wheelbase of the van

$L_t = e + f$ = Wheelbase of the trailer (hitch to wheels)

$\zeta = W_b/W$ = Nondimensional weight of the trailer

Then solving the equation for Θ, we obtain the gradeability expression for the case of:

FWD

$$\Theta = \mu \frac{\frac{c}{L} - \zeta \frac{d}{L} \frac{f}{L_t}}{1 + \mu \frac{h}{L} + \zeta \left(1 + \mu \frac{h_2}{L} + \mu \frac{d}{L} \frac{h_2 - h_3}{L_t}\right)}$$

The numerator represents the static weight on the front axle, due to the weight of the van diminished by the vertical load of the trailer on the hitch (the hitch load decreases the front axle load, and hence the gradeability). The second term in the denominator reflects the effect of longitudinal transfer of load from the front axle on a grade due to the elevated position of the CG on the van. The terms in parentheses in the denominator represent the effects of the trailer. The first term in parentheses is the direct effect of the added weight of the trailer. The next term arises from the longitudinal transfer of load off of the front axle due to the towing force at the hitch. The last term is the effect of the change in vertical load on the hitch due to the tow force.

A similar analysis produces a different solution for the case of:

RWD

$$\Theta = \mu \frac{\frac{b}{L} + \zeta \frac{(L + d)}{L} \frac{f}{L_t}}{1 - \mu \frac{h}{L} + \zeta \left(1 - \mu \frac{h_2}{L} - \mu \frac{(L + d)}{L} \frac{h_2 - h_3}{L_t}\right)}$$

On the rear-wheel drive, static load of the trailer (second term in the numerator) increases gradeability because it increases load on the drive wheels. In the denominator, the terms representing longitudinal load transfer are negative (thereby decreasing the magnitude of the denominator and increasing the gradeability).

Finally, in the case of four-wheel drive, the performance that will be obtained depends on the type of drive system. The most effective utilizes a limited-slip differential on each axle and a limited-slip interaxle drive, so that the torque is distributed to all the wheels in proportion to their traction. Then the van can develop a traction force that is the coefficient of friction times its weight.

$$(W + W_b) \tan\Theta = \mu W$$

or:

$$\Theta = \mu \frac{W}{W + W_b} = \mu \frac{1}{1 + \zeta}$$

For four-wheel-drive systems that do not have full limited-slip features, the solution would require a more complex treatment based on an analysis of the drive forces that would be available from the individual axles.

Example calculations:

For the parameters given in the problem the solutions are:

FWD $\Theta = 0.1018 = 10.18$ % slope = 5.84 deg

RWD $\Theta = 0.1142 = 11.42$ % slope = 6.51 deg

4WD $\Theta = 0.1944 = 19.44$ % slope = 11.0 deg

Despite the fact that the assumed vehicle has a greater static load on the front axle (57% of the weight), the RWD configuration has better gradeability because of the longitudinal transfer of load on the grade.

REFERENCES

1. Roberts, P., Collector's History of the Automobile, Bonanza Books, New York, N.Y., 1978, 320 p.
2. Encyclopedia Americana, Vol. 2, 1966, 645 p.
3. American Cars Since 1775, Automobile Quarterly, Inc., New York, 1971, 504 p.
4. Olley, M., "Reminiscences - Feb 16/57," unpublished, 1957, 17 p.
5. Lanchester, F.W., "Some Reflections Peculiar to the Design of an Automobile," Proceedings of the Institution of Automobile Engineers, Vol. 2, 1908, pp.187-257.
6. Segel, L.,"Some Reflections on Early Efforts to Investigate the Directional Stability and Control of the Motor Car," unpublished, 1990, 7 p.
7. Broulhiet, G., "La Suspension de la Direction de la Voiture Automobile: Shimmy et Dandinement," *Societe des Ingenieurs Civils de France Bulletin*, Vol. 78, 1925.
8. Lanchester, F.W., "Automobile Steering Gear—Problems and Mechanism," Proceedings of the Institution of Automobile Engineers, Vol. 22, 1928, pp. 726-41.
9. Becker, G., *et al.*, "Schwingungen in Automobillernkung," Krayn Berlag, Berlin, 1931.
10. Lanchester, F.W., "Motor Car Suspension and Independent Springing," Proceedings of the Institution of Automobile Engineers, Vol. 30, 1936, pp. 668-762.

11. Olley, M., "Independent Wheel Suspensions—Its Whys and Wherefores," Society of Automotive Engineers Journal, Vol. 34, No. 3, 1934, pp. 73-81.
12. Rieckert, P., and Schunk, T.E., "Zur Fahrmechanik des Gummibereiften Kraftfahrzeugs," *Ingenieur Archiv*, Vol. 11, 1940.
13. Rocard, Y., "Les Mefaits du Roulement, Auto-Oscillations et Instabilite de Route," *La Revue Scientifique*, Vol. 84, No. 45, 1946.
14. Segel, L., "Research in the Fundamentals of Automobile Control and Stability," Transactions of the Society of Automotive Engineers, Vol. 65, 1956, pp. 527-40.
15. Ellis, J.R., Vehicle Dynamics, Business Books Limited, London, 1969, 243 p.
16. Ellis, J.R., Road Vehicle Dynamics, John R. Ellis, Inc., Akron, OH, 1988, 294 p.
17. Wong, J.C., Theory of Ground Vehicles, John Wiley & Sons, New York, 1978, 330 p.
18. Fundamentals of Vehicle Dynamics, General Motors Institute, Flint, MI.
19. Cole, D., "Elementary Vehicle Dynamics," course notes in Mechanical Engineering, The University of Michigan, Ann Arbor, MI, 1972.
20. Fitch, J.W., Motor Truck Engineering Handbook (Third Edition), James W. Fitch, publisher, Anacortes, WA, 1984, 288 p.
21. Newton, K., Steeds, W., and Garrett, T.K., The Motor Vehicle (Tenth Edition), Butterworths, London, 1983, 742 p.
22. Automotive Handbook, 2nd Ed., Robert Bosch GmbH, Stuttgart, 1986, 707 p.
23. Bastow, D., Car Suspension and Handling, Second Edition, Pentech Press, London, 1990, 300 p.
24. Goodsell, D., Dictionary of Automotive Engineering, Butterworths, London, 1989, 182 p.
25. "Vehicle Dynamics Terminology," SAE J670e, Society of Automotive Engineers, Warrendale, PA (see Appendix A).
26. Den Hartog, J.P., Mechanics, McGraw-Hill Book Company, Inc., New York, NY, 1948, p. 174.

CHAPTER 2
ACCELERATION PERFORMANCE

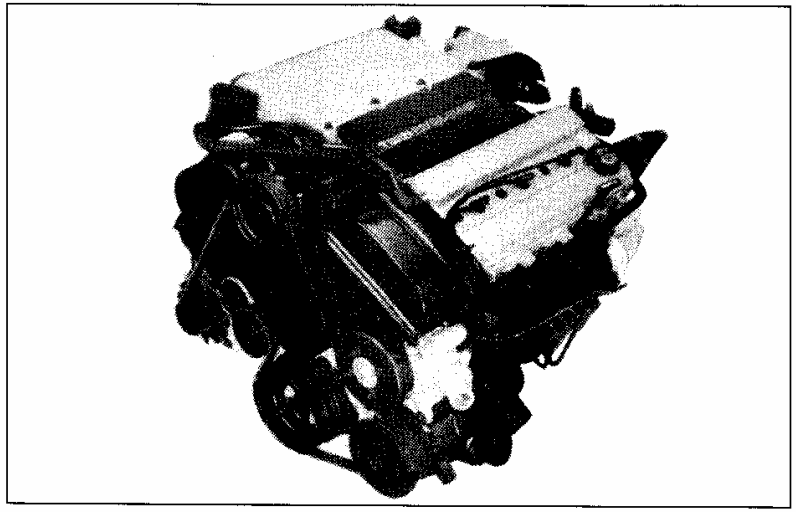

3.4L Twin Dual Cam V6. (Photo courtesy of General Motors Corp.)

Maximum performance in longitudinal acceleration of a motor vehicle is determined by one of two limits—engine power or traction limits on the drive wheels. Which limit prevails may depend on vehicle speed. At low speeds tire traction may be the limiting factor, whereas at high speeds engine power may account for the limits.

POWER-LIMITED ACCELERATION

The analysis of power-limited acceleration involves examination of the engine characteristics and their interaction through the power train.

Engines

The source of propulsive power is the engine. Engines may be characterized by their torque and power curves as a function of speed. Figure 2.1 shows typical curves for gasoline and diesel engines. Gasoline engines typically have a torque curve that peaks in the mid-range of operating speeds controlled by the

induction system characteristics. In comparison, diesel engines may have a torque curve that is flatter or even rises with decreasing speed. This characteristic, controlled by the programming of the injection system, has led to the high-torque-rise heavy-duty engines commonly used in commercial vehicles. (In some cases the torque rise may be so great as to provide nearly constant power over much of the engine operating speed range.)

The other major difference between the two types of engines is the specific fuel consumption that is obtained. At their most efficient, gasoline engines may achieve specific fuel consumption levels in the range near 0.4 lb/hp-hr, whereas diesels may be near 0.2 or lower.

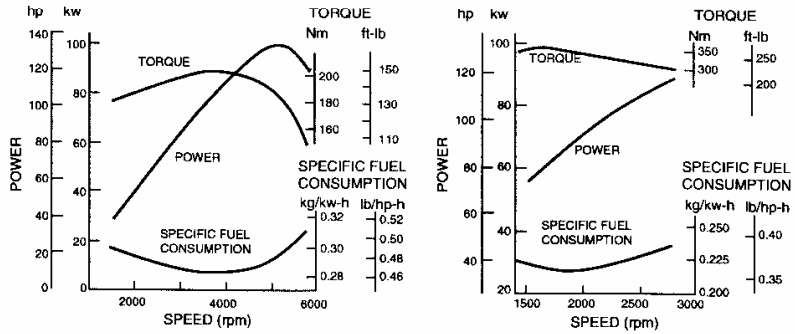

Fig. 2.1 Performance characteristics of gasoline and diesel engines.

Power and torque are related by the speed. Specifically,

Power (ft-lb/sec) = Torque (ft-lb) x speed (radians/sec)

$$\text{Horsepower} = T\ (\text{ft-lb}) \times \omega_e\ (\text{rad/sec}) / 550 = T\ (\text{ft-lb}) \times \text{RPM} / 5252 \qquad (2\text{-}1)$$

Also,

$$\text{Power (kw)} = 0.746 \times \text{HP} \qquad 1\ \text{hp} = 550\ \text{ft-lb/sec} \qquad (2\text{-}2)$$

The ratio of engine power to vehicle weight is the first-order determinant of acceleration performance. At low to moderate speeds an upper limit on acceleration can be obtained by neglecting all resistance forces acting on the vehicle. Then from Newton's Second Law:

$$M\,a_x = F_x \qquad (2\text{-}3)$$

where:

M = Mass of the vehicle = W/g
a_x = Acceleration in the forward direction
F_x = Tractive force at the drive wheels

Since the drive power is the tractive force times the forward speed, Eq. (2-3) can be written:

$$a_x = \frac{1}{M} F_x = 550 \frac{g}{V} \frac{HP}{W} \quad (ft/sec^2) \qquad (2\text{-}4)$$

where:

g = Gravitational constant (32.2 ft/sec^2)
V = Forward speed (ft/sec)
HP = Engine horsepower
W = Weight of the vehicle (lb)

Because of the velocity term in the denominator, acceleration capability must decrease with increasing speed. The general relationship of the above equation is shown in Figure 2.2 for cars and trucks. As might be expected, heavy trucks will have much lower performance levels than cars because of the less favorable power-to-weight ratio. Although this is a very simple representation of acceleration performance, it is useful to highway engineers responsible for establishing highway design policies with respect to the needs for climbing lanes on long upgrades, sight distances at intersections, and acceleration areas on entrance ramps [1].

Power Train

More exact estimation of acceleration performance requires modeling the mechanical systems by which engine power is transmitted to the ground. Figure 2.3 shows the key elements.

Starting with the engine, it must be remembered that engine torque is measured at steady speed on a dynamometer, thus the actual torque delivered to the drivetrain is reduced by the amount required to accelerate the inertia of the rotating components (as well as accessory loads not considered here). The torque delivered through the clutch as input to the transmission can be determined by application of NSL as:

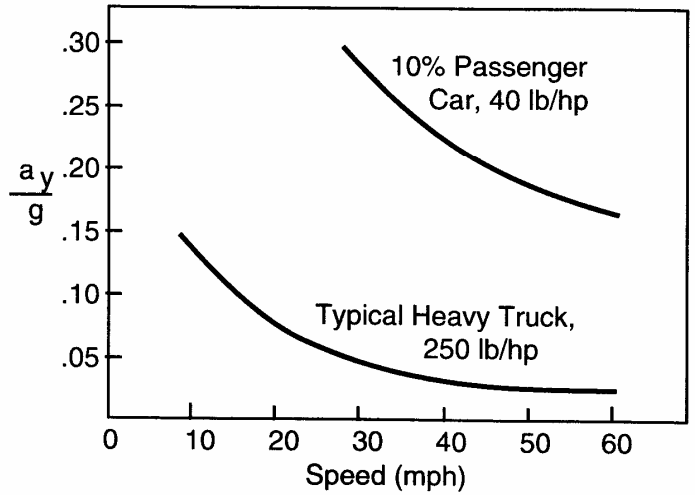

Fig. 2.2 Effect of velocity on acceleration capabilities of cars and trucks [2].

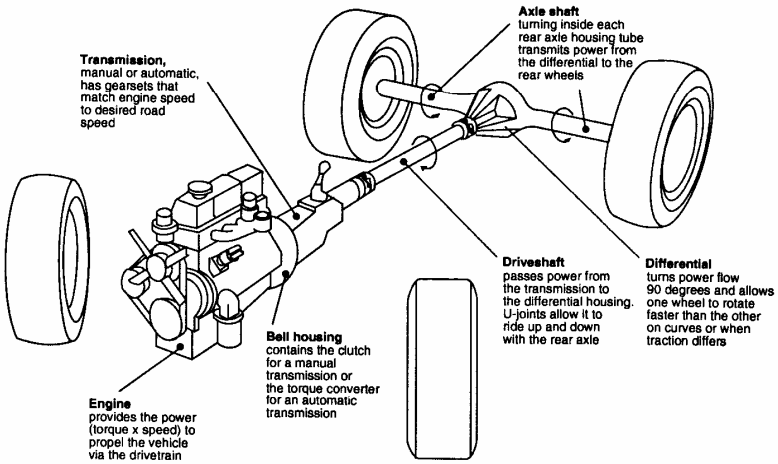

Fig. 2.3 Primary elements in the power train.

$$T_c = T_e - I_e \alpha_e \qquad (2\text{-}5)$$

where:

T_c = Torque at the clutch (input to the transmission)
T_e = Engine torque at a given speed (from dynamometer data)
I_e = Engine rotational inertia
α_e = Engine rotational acceleration

The torque delivered at the output of the transmission is amplified by the gear ratio of the transmission but is decreased by inertial losses in the gears and shafts. If the transmission inertia is characterized by its value on the input side, the output torque can be approximated by the expression:

$$T_d = (T_c - I_t \alpha_e) N_t \qquad (2\text{-}6)$$

where:

T_d = Torque output to the driveshaft
N_t = Numerical ratio of the transmission
I_t = Rotational inertia of the transmission (as seen from the engine side)

Similarly, the torque delivered to the axles to accelerate the rotating wheels and provide tractive force at the ground is amplified by the final drive ratio with some reduction from the inertia of the driveline components between the transmission and final drive. The expression for this is:

$$T_a = F_x r + I_w \alpha_w = (T_d - I_d \alpha_d) N_f \qquad (2\text{-}7)$$

where:

T_a = Torque on the axles
F_x = Tractive force at the ground
r = Radius of the wheels
I_w = Rotational inertial of the wheels and axles shafts
α_w = Rotational acceleration of the wheels
I_d = Rotational inertia of the driveshaft
α_d = Rotational acceleration of the driveshaft
N_f = Numerical ratio of the final drive

Now the rotational accelerations of the engine, transmission, and driveline are related to that of the wheels by the gear ratios.

$$\alpha_d = N_f \alpha_w \quad \text{and} \quad \alpha_e = N_t \alpha_d = N_t N_f \alpha_w \qquad (2\text{-}8)$$

The above equations (2-5) to (2-8) can be combined to solve for the tractive force available at the ground. Recognizing that the vehicle acceleration, a_x, is the wheel rotational acceleration, α_w, times the tire radius, yields:

$$F_x = \frac{T_e N_{tf}}{r} - \{(I_e + I_t) N_{tf}^2 + I_d N_f^2 + I_w\} \frac{a_x}{r^2} \qquad (2\text{-}9a)$$

where:

N_{tf} = Combined ratio of transmission and final drive

Thus far the inefficiencies due to mechanical and viscous losses in the driveline components (transmission, driveshaft, differential and axles) have not been taken into account. These act to reduce the engine torque in proportion to the product of the efficiencies of the individual components [3]. The efficiencies vary widely with the torque level in the driveline because viscous losses occur even when the torque is zero. As a rule of thumb, efficiencies in the neighborhood of 80% to 90% are typically used to characterize the driveline [5]. The effect of mechanical losses can be approximated by adding an efficiency value to the first term on the right-hand side of the previous equation, giving:

$$F_x = \frac{T_e N_{tf} \eta_{tf}}{r} - \{(I_e + I_t) N_{tf}^2 + I_d N_f^2 + I_w\} \frac{a_x}{r^2} \qquad (2\text{-}9b)$$

where:

η_{tf} = Combined efficiency of transmission and final drive

Thus Eq. (2-9b) provides an expression for the tractive force that can be obtained from the engine. It has two components:

1) The first term on the right-hand side is the engine torque multiplied by the overall gear ratio and the efficiency of the drive system, then divided by tire radius. This term represents the steady-state tractive force available at the ground to overcome the road load forces of aerodynamics and rolling resistance, to accelerate, or to climb a grade.

2) The second term on the right-hand side represents the "loss" of tractive force due to the inertia of the engine and drivetrain components. The term in brackets indicates that the equivalent inertia of each component is "amplified" by the square of the numerical gear ratio between the component and the wheels.

Knowing the tractive force, it is now possible to predict the acceleration performance of a vehicle. The expression for the acceleration must consider all the forces that were shown in Figure 1.6. The equation takes the form:

$$M a_x = \frac{W}{g} a_x = F_x - R_x - D_A - R_{hx} - W \sin \Theta \qquad (2\text{-}10)$$

where:

M = Mass of the vehicle = W/g
a_x = Longitudinal acceleration (ft/sec^2)
F_x = Tractive force at the ground (Eq. (2-9b))
R_x = Rolling resistance forces
D_A = Aerodynamic drag force
R_{hx} = Hitch (towing) forces

F_x includes the engine torque and rotational inertia terms. As a convenience, the rotational inertias from Eq. (2-9b) are often lumped in with the mass of the vehicle to obtain a simplified equation of the form:

$$(M + M_r)\, a_x = \frac{W + W_r}{g} a_x = \frac{T_e N_{tf} \eta_{tf}}{r} - R_x - D_A - R_{hx} - W \sin \Theta \qquad (2\text{-}11)$$

where:

M_r = Equivalent mass of the rotating components

The combination of the two masses is an "effective mass," and the ratio of $(M + M_r)/M$ is the "mass factor." The mass factor will depend on the operating gear, with typical values as below:

		Mass Factor			
Vehicle	Gear:	High	Second	First	Low
Small Car		1.11	1.20	1.50	2.4
Large Car		1.09	1.14	1.30	—
Truck		1.09	1.20	1.60	2.5

A representative number is often taken as [4]:

$$\text{Mass Factor} = 1 + 0.04 + 0.0025\, N_{tf}^2 \qquad (2\text{-}12)$$

In the complete form of Eq. (2-11), there are no convenient explicit solutions for acceleration performance. Except for the grade term, all other forces vary with speed, and must be evaluated at each speed. An equation as shown above can be used to calculate acceleration performance by hand for a few speeds, but when repeated calculations are required (for example, to calculate acceleration from zero to a high speed), programming on a computer is most often the preferred method [6, 7, 8].

The tractive force generated by the engine/power train (the first term on the right side of Eq. (2-11)) is the effort available to overcome road load forces and accelerate the vehicle. This is shown for a four-speed manual transmission in Figure 2.4.

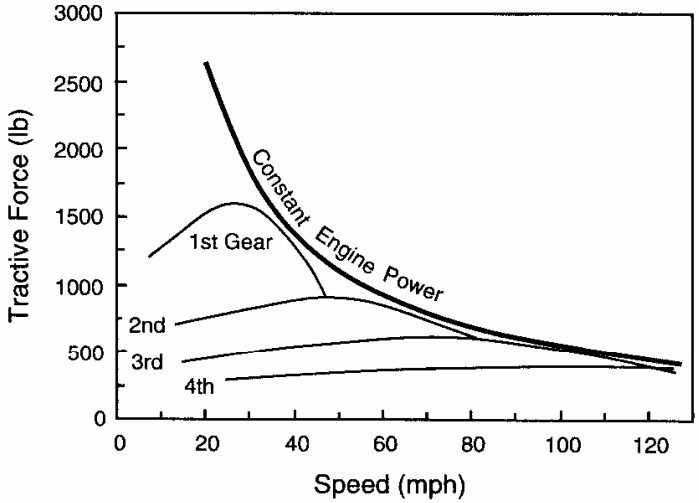

Fig. 2.4 Tractive effort-speed characteristics for a manual transmission.

The "Constant Engine Power" line is equal to the maximum power of the engine, which is the upper limit of tractive effort available, less any losses in the driveline. It is only approached when the engine reaches the speed at which it develops maximum power. The tractive force line for each gear is the image of the engine torque curve multiplied by the ratios for that gear. The curves illustrate visually the need to provide a number of gear ratios for operation of the vehicle (low gearing for start-up, and high gearing for high-speed driving).

For maximum acceleration performance the optimum shift point between gears is the point where the lines cross. The area between the lines for the different gears and the constant power curve is indicative of the deficiencies of the transmission in providing maximum acceleration performance.

Automatic Transmissions

Automatic transmissions provide somewhat different performance, more closely matching the ideal because of the torque converter on the input. Torque converters are fluid couplings that utilize hydrodynamic principles to amplify the torque input to the transmission at the expense of speed. Figure 2.5 shows the torque ratio and efficiency characteristics of a typical torque converter as a function of speed ratio (output/input speed). At zero output speed (speed ratio of zero) the output torque will be several times that of the input. Thus the torque

input to the transmission will be twice the torque coming out of the engine when the transmission is stalled, providing for good "off-the-line" acceleration performance. As speed builds up and the transmission input approaches engine speed, the torque ratio drops to unity.

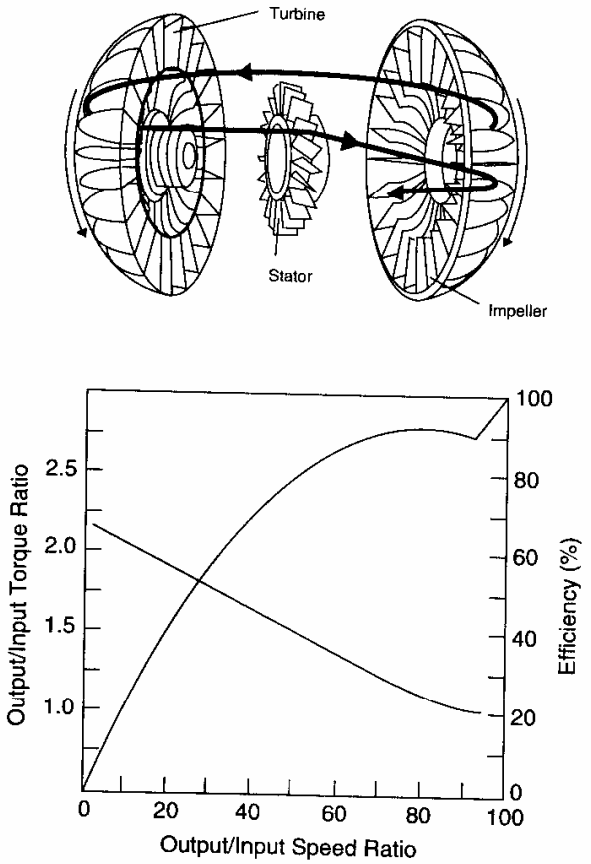

Fig. 2.5 Characteristics of a typical torque converter.

The torque amplification provides for more favorable tractive effort-speed performance as shown for a four-speed automatic transmission in Figure 2.6. Because of the slip possible with the fluid coupling, the torque curves in each gear can extend down to zero speed without stalling the engine. At low speed

in first gear the effect of the torque converter is especially evident as the tractive effort rises down toward the zero speed condition.

Also shown on this figure are the road load forces arising from rolling resistance, aerodynamic drag, and road grade (0, 5, 10, 15 and 20%). At a given speed and gear the difference between the tractive effort curve and the appropriate road load curve is the tractive force available to accelerate the vehicle (and its rotating components). The intersection between the road load curves and any of the tractive effort curves is the maximum speed that can be sustained in that gear.

The actual ratios selected for a transmission may be tailored for performance in specific modes—an optimal first gear for starting, a second or third gear for passing, and a high gear for fuel economy at road speeds. The best gear ratios usually fall close to a geometric progression, in which the ratios change by a constant percentage from gear to gear. Figure 2.7 illustrates the relationship of engine speed to road speed obtained with geometric progression. Figure 2.8 shows the engine-road speed relationship for an actual production car. Note that although it is close to geometric progression, some variation occurs.

In these times the choices made in selection of transmission gear ratios must also reflect the realities of the pressures for fuel economy and emissions. The engine performance in both of these respects is quantified by mapping its characteristics. An example of a fuel consumption map for a V-8 engine is

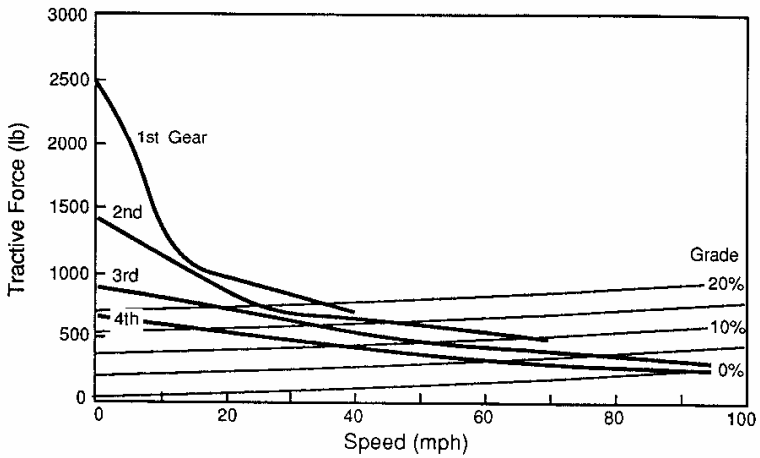

Fig. 2.6 Tractive effort-speed characteristics for an automatic transmission.

shown in Figure 2.9. The figure shows lines of constant fuel consumption (pounds per brake-horsepower-hour) as a function of brake-mean-effective-pressure (indicative of torque) and engine speed. Near the boundaries the specific fuel consumption is highest. In the middle is a small island of minimum fuel consumption at the rate of 0.46 lb/bhp-hr. To maximize

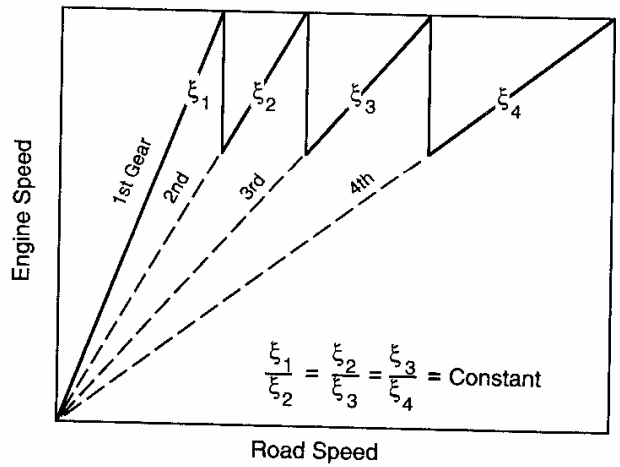

Fig. 2.7 Selection of gear ratios based on geometric progression.

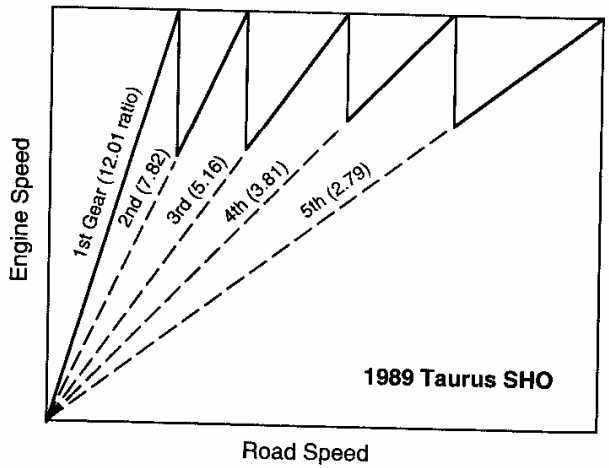

Fig. 2.8 Gear ratios on a typical passenger car.

highway fuel economy the vehicle and driveline should be designed to operate in this region. For best economy over the full driving range the transmission should be designed to operate along the bold line which stays within the valleys of minimum fuel consumption over the broadest range of engine speeds.

For emissions purposes, similar maps of engine performance can be developed to characterize the emissions properties, and a similar logic would be used to identify transmission characteristics that would minimize emissions.

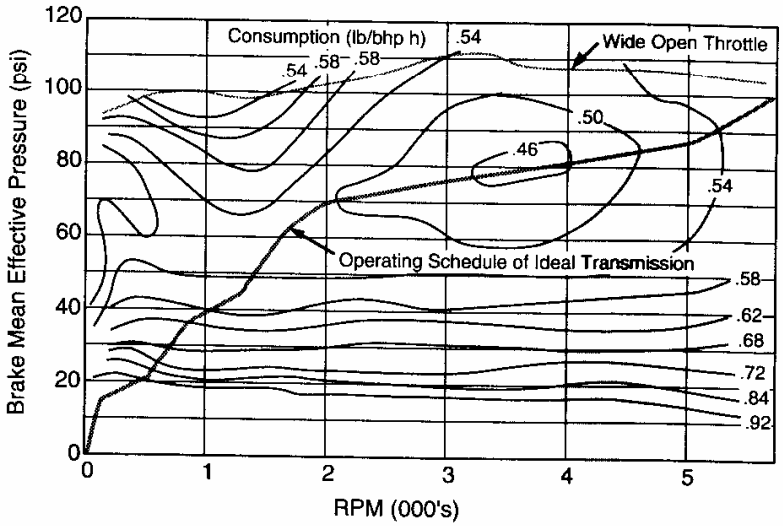

Fig. 2.9 Specific fuel consumption map of a V-8 engine (300 cubic inch).

EXAMPLE PROBLEMS

1) We are given the following information about the engine and drivetrain components for a passenger car:

Engine inertia	0.8 in-lb-sec^2					
RPM/Torque (ft-lb)	800	120	2400	175	4000	200
	1200	132	2800	181	4400	201
	1600	145	3200	190	4800	198
	2000	160	3600	198	5200	180

Transmission Data - Gear	1	2	3	4	5
Inertias	1.3	0.9	0.7	0.5	0.3 in-lb-sec^2
Ratios	4.28	2.79	1.83	1.36	1.00
Efficiencies	0.966	0.967	0.972	0.973	0.970

Final drive -		
	Inertia	1.2 in-lb-sec^2
	Ratio	2.92
	Efficiency	0.99

Wheel inertias Drive 11.0 in-lb-sec^2 Non-drive 11.0 in-lb-sec^2

Wheel size 801 rev/mile $\Rightarrow$ 6.59 ft circumference $\Rightarrow$ 12.59 inch radius

a) Calculate the effective inertia of the drivetrain components in first gear.

Solution:

The effective inertia is given by the second term on the right-hand side of Eq.(2-9b), which had the following form:

$$F_x = \frac{T_e N_{tf} \eta_{tf}}{r} - \{(I_e + I_t) N_{tf}^2 + I_d N_f^2 + I_w\} \frac{a_x}{r^2} \qquad (2\text{-}9b)$$

The term in the brackets is the effective inertia. It is calculated as follows:

$$I_{eff} = \{(I_e + I_t)(N_{tf})^2 + I_d N_f^2 + I_w\}$$
$$= (0.8 + 1.3) \text{ in-lb-sec}^2 (4.28 \times 2.92)^2 + 1.2 \times 2.92^2 + 2 \times 11.0 \text{ in-lb-sec}^2$$
$$= 328 + 10.2 + 22 = 360.2 \text{ in-lb-sec}^2$$

Notes:

1) The engine and first gear components are the largest inertia when operating in first gear. In fifth gear, the inertia of these components is about 9.7 in-lb-sec^2.

2) Only the inertia of the drive wheels was included in this solution because only they subtract from the tractive force available at the ground at the drive wheels. We must keep in mind that the non-driven wheels contribute an additional inertia when the vehicle is accelerated. The inertia of the non-driven wheels should be lumped in with the inertia (mass) of the total vehicle.

3) The rotational inertia, in units of in-lb-sec^2, is converted into translational inertia (mass) when divided by r^2 in Eq. (2-9). We can see its magnitude as follows:

$$M_{eff} = I_{eff} / r^2 = 360.2 \text{ in-lb-sec}^2 / 12.59^2 \text{ in}^2 = 2.27 \text{ lb-sec}^2/\text{in}$$

Perhaps the more familiar form is the effective weight:

$$W_{eff} = M_{eff}\, g = 2.27 \text{ lb-sec}^2/\text{in} \times 386 \text{ in/sec}^2 = 877 \text{ lb}$$

Comparing this figure to the weight of a typical passenger car (2500 lb), we see that it adds about 35% to the effective weight of the car during acceleration in first gear. The inertia of the non-driven wheels will add another 27 lb to the effective weight (1%).

2) Calculate the maximum tractive effort and corresponding road speed in first and fifth gears of the car described above when inertial losses are neglected.

Solution:

Maximum tractive effort will coincide with maximum torque, which occurs at 4400 rpm. So the problem reduces to finding the tractive effort from the first term in Eq. (2-9) for that value of torque.

$$F_x = T_e N_{tf} \eta_{tf} / r$$
$$= 201 \text{ ft-lb } (4.28 \times 2.92)\ (0.966 \times 0.99)/12.59 \text{ in} \times 12 \text{ in/ft}$$
$$= 2290 \text{ lb}$$

The road speed is determined by use of the relationships given in Eq. (2-8). Although the equation is written in terms of acceleration, the same relationships hold true for speed. That is:

$$\omega_d = N_f \omega_w \quad \text{and} \quad \omega_e = N_t \omega_d = N_t N_f \omega_w \qquad (2\text{-}8a)$$

The wheel rotational speed will be:

$$\omega_w = \omega_e / (N_t N_f) = 4400 \text{ rev/min} \cdot 2\pi \text{ rad/rev} \cdot 1 \text{ min/60 sec} / (4.28 \times 2.92)$$
$$= 36.87 \text{ rad/sec}$$

The corresponding ground speed will be found by converting the rotational speed to translational speed at the circumference of the tire.

$$V_x = \omega_w \cdot r = 36.87 \text{ rad/sec} \times 12.59 \text{ in} = 464.2 \text{ in/sec} = 38.7 \text{ ft/sec} = 26.4 \text{ mph}$$

The same method is used to calculate performance in high gear as well:

$F_x = T_e N_{tf} \eta_{tf}/r$

$= 201$ ft-lb (1.0 x 2.92) (0.99 x 0.97)/12.59 in x 12 in/ft

$= 537$ lb

$\omega_w = \omega_e/(N_t N_f) = 4400$ rev/min $\cdot 2\pi$ rad/rev $\cdot$ 1 min/60 sec /(1.0 x 2.92)

$= 157.8$ rad/sec

$V_x = \omega_w \cdot r = 157.8$ rad/sec x 12.59 in $= 1987$ in/sec $= 165$ ft/sec $= 113$ mph

TRACTION-LIMITED ACCELERATION

Presuming there is adequate power from the engine, the acceleration may be limited by the coefficient of friction between the tire and road. In that case F_x is limited by:

$$F_x = \mu W \qquad (2\text{-}13)$$

where:

μ = Peak coefficient of friction

W = Weight on drive wheels

The weight on a drive wheel then depends on the static plus the dynamic load due to acceleration, and on any transverse shift of load due to drive torque.

Transverse Weight Shift due to Drive Torque

Transverse weight shift occurs on all solid drive axles, whether on the front or rear of the vehicle. The basic reactions on a rear axle are shown in Figure 2.10. The driveshaft into the differential imposes a torque T_d on the axle. As will be seen, the chassis may roll compressing and extending springs on opposite sides of the vehicle such that a torque due to suspension roll stiffness, T_s, is produced. Any difference between these two must be absorbed as a difference in weight on the two wheels. If the axle is of the non-locking type, then the torque delivered to both wheels will be limited by the traction limit on the most lightly loaded wheel.

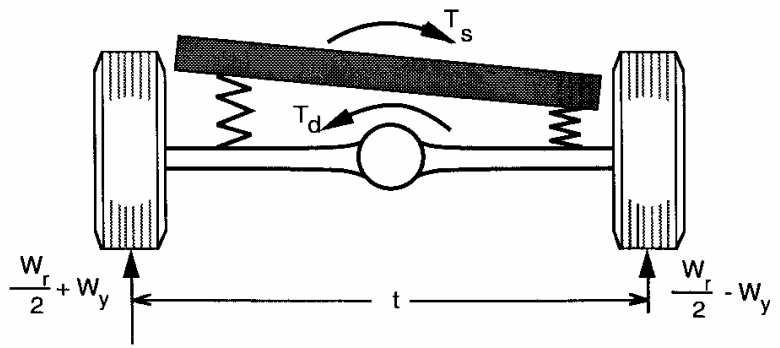

Fig. 2.10. Free-body diagram of a solid drive axle.

Writing NSL for rotation of the axle about its centerpoint allows the reactions to be related. When the axle is in equilibrium:

$$\Sigma T_o = (W_r/2 + W_y - W_r/2 + W_y)\, t/2 + T_s - T_d = 0 \qquad (2\text{-}14)$$

or $W_y = (T_d - T_s)/t$

In the above equation, T_d can be related to the drive forces because:

$$T_d = F_x r/N_f \qquad (2\text{-}15)$$

where:

F_x = Total drive force from the two rear wheels

r = Tire radius

N_f = Final drive ratio

However, it is necessary to determine the roll torque produced by the suspension, which requires an analysis of the whole vehicle because the reaction of the drive torque on the chassis attempts to roll the chassis on both the front and rear suspensions. The entire system of interest is illustrated in Figure 2.11 for the case of a rear-wheel-drive car.

The drive torque reaction at the engine/transmission is transferred to the frame and distributed between the front and rear suspensions. It is generally assumed that the roll torque produced by a suspension is proportional to roll angle (Hooke's Law) of the chassis. Then:

$$T_{sf} = K_{\phi f}\,\phi \tag{2-16a}$$

$$T_{sr} = K_{\phi r}\,\phi \tag{2-16b}$$

$$K_{\phi} = K_{\phi f} + K_{\phi r} \tag{2-16c}$$

where:

T_{sf} = Roll torque on the front suspension

T_{sr} = Roll torque on the rear suspension

$K_{\phi f}$ = Front suspension roll stiffness

$K_{\phi r}$ = Rear suspension roll stiffness

K_{ϕ} = Total roll stiffness

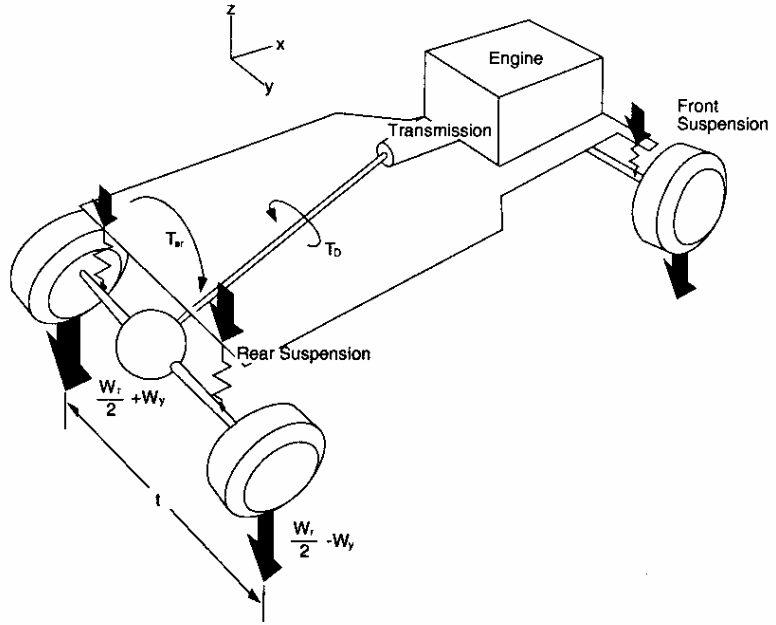

Fig. 2.11 Diagram of drive torque reactions on the chassis.

Now T_{sr} can be related to the roll angle, and the roll angle can be related to the drive torque as follows. The roll angle is simply the drive torque divided by the total roll stiffness:

$$\phi = T_d / K_\phi = T_d / (K_{\phi f} + K_{\phi r}) \tag{2-17}$$

Therefore, substituting in Eq. (2-16b):

$$T_{sr} = K_{\phi r} T_d / (K_{\phi f} + K_{\phi r})$$

This in turn can be substituted into Eq. (2-14), along with the expression for T_d obtained from Eq. (2-15):

$$W_y = \frac{F_x r}{N_f t} \left[1 - \frac{K_{\phi r}}{K_{\phi r} + K_{\phi f}} \right] \tag{2-18a}$$

The term in the brackets collapses to yield:

$$W_y = \frac{F_x r}{N_f t} \frac{K_{\phi f}}{K_\phi} \tag{2-18b}$$

This equation gives the magnitude of the lateral load transfer as a function of the tractive force and a number of vehicle parameters such as the final drive ratio, tread of the axle, tire radius, and suspension roll stiffnesses. The net load on the rear axle during acceleration will be its static plus its dynamic component (see Eq. (1-7)). For a rear axle:

$$W_r = W\left(\frac{b}{L} + \frac{a_x}{g}\frac{h}{L}\right) \tag{2-19}$$

Neglecting the rolling resistance and aerodynamic drag forces, the acceleration is simply the tractive force divided by the vehicle mass.

$$W_r = W\left(\frac{b}{L} + \frac{F_x}{M g}\frac{h}{L}\right) \tag{2-20}$$

Then the weight on the right rear wheel, W_{rr}, will be $W_r/2 - W_y$, or:

$$W_{rr} = \frac{W b}{2 L} + \frac{F_x}{2}\frac{h}{L} - \frac{F_x r}{N_f t}\frac{K_{\phi f}}{K_\phi} \tag{2-21}$$

and

$$F_x = 2\mu W_{rr} = 2\mu \left(\frac{W b}{2 L} + \frac{F_x h}{2 L} - \frac{F_x r}{N_f t}\frac{K_{\phi f}}{K_\phi}\right) \tag{2-22}$$

Traction Limits

Solving for F_x gives the final expression for the maximum tractive force that can be developed by a solid rear axle with a non-locking differential:

$$F_{xmax} = \frac{\mu \frac{W b}{L}}{1 - \frac{h}{L}\mu + \frac{2\mu r}{N_f t}\frac{K_{\phi f}}{K_\phi}} \tag{2-23}$$

For a solid rear axle with a locking differential, additional tractive force can be obtained from the other wheel up to its traction limits such that the last term in the denominator of the above equation drops out. This would also be true in the case of an independent rear suspension because the driveline torque reaction is picked up by the chassis-mounted differential. In both of these cases the expression for the maximum tractive force is:

$$F_{xmax} = \frac{\mu \frac{W b}{L}}{1 - \frac{h}{L}\mu} \tag{2-24}$$

Finally, in the case of a front axle, the fore/aft load transfer is opposite from the rear axle case. Since the load transfer is reflected in the second term of the denominator, the opposite direction yields a sign change. Also, the term "W b/L" arose in the earlier equations to represent the static load on the rear drive axle. For a front-wheel-drive vehicle the term becomes "W c/L." For the solid front drive axle with non-locking differential:

$$F_{xmax} = \frac{\mu \frac{W c}{L}}{1 + \frac{h}{L}\mu + \frac{2\mu r}{N_f t}\frac{K_{\phi r}}{K_\phi}} \tag{2-25}$$

And for the solid front drive axle with locking differential, or the independent front drive axle as typical of most front-wheel-drive cars today:

$$F_{xmax} = \frac{\mu \frac{W c}{L}}{1 + \frac{h}{L}\mu} \tag{2-26}$$

EXAMPLE PROBLEMS

1) Find the traction-limited acceleration for the rear-drive passenger car with and without a locking differential on a surface of moderate friction level. The information that will be needed is as follows:

Weights	Front - 2100 lb	Rear - 1850 lb	Total - 3950 lb
CG height	21.0 in	Wheelbase - 108 in	
Coefficient of friction	0.62	Tread - 59.0 in	
Final drive ratio	2.90	Tire size - 13.0 in	
Roll stiffnesses	Front - 1150 ft-lb/deg	Rear - 280 ft-lb/deg	

Solution:

The equation for the maximum tractive force of a solid axle rear-drive vehicle with a non-locking differential was given in Eq. (2-23):

$$F_{xmax} = \frac{\mu \frac{Wb}{L}}{1 - \frac{h}{L}\mu + \frac{2\mu r}{N_f t}\frac{K_{\phi f}}{K_\phi}} \qquad (2\text{-}23)$$

In this equation, W b/L is just the rear axle weight, which is known; therefore we do not have to find the value for the parameter "b." Likewise, all the other terms are known and can be substituted into the equation to obtain:

$$F_{xmax} = \frac{(0.62)\ 1850\ \text{lb}}{1 - \frac{21}{108}0.62 + \frac{2}{2.9}\frac{(0.62)}{59\ \text{in}}\frac{13\ \text{in}\ 1150}{1430}}$$

$$= \frac{1147\ \text{lb}}{1 - 0.121 + 0.0758} = \frac{1147}{0.9548} = 1201\ \text{lb}$$

$$a_x = \frac{F_{xmax}}{M\,g} = \frac{1201\ \text{lb}}{3950\ \text{lb}} = 0.3041\ \text{g's} = 9.79\ \frac{\text{ft}}{\text{sec}^2}$$

With a locking differential the third term in the denominator disappears (Eq. (2-24)) so that we obtain:

$$F_{xmax} = \frac{(0.62)\ 1850\ \text{lb}}{1 - \frac{21}{108}0.62} = \frac{1147\ \text{lb}}{1 - 0.121} = \frac{1147}{0.879} = 1305\ \text{lb}$$

$$a_x = \frac{F_{xmax}}{M\,g} = \frac{1305\ \text{lb}}{3950\ \text{lb}} = 0.330\ \text{g's} = 10.64\ \frac{\text{ft}}{\text{sec}^2}$$

Notes:

a) For both cases the numerator term is the weight on the drive axle times the coefficient of friction which is equivalent to 1147 lb of tractive force.

b) Similarly, the dynamic load transfer onto the rear (drive) axle from acceleration is accounted for by the second term in the denominator which diminishes the magnitude of the denominator by 12.1%, thereby increasing the tractive force by an equivalent percentage.

c) The lateral load transfer effect appears in the third term of the denominator, increasing its value by approximately 7.6%, which has the effect of decreasing the tractive force by about the same percentage. Comparing the two answers, the loss from lateral load transfer on the drive axle with a non-locking differential is 104 lb. On higher friction surfaces a higher loss would be seen.

2) Find the traction-limited performance of a front-wheel-drive vehicle under the same road conditions as the problem above. The essential data are:

Weights	Front - 1950	Rear - 1150	Total - 3100
CG Height	19.0 in	Wheelbase - 105 in	
Coefficient of friction	0.62	Tread - 60 inches	
Final drive ratio	3.70	Tire size - 12.59 inches	
Roll stiffnesses	Front - 950 ft-lb/deg	Rear - 620 ft-lb/deg	

Solution:

Most front-wheel-drive vehicles have an independent front suspension. Thus the equation for maximum tractive effort is given by Eq. (2-26), and we notice that all the data required to calculate lateral load transfer on the axle are not needed. The maximum tractive force is calculated by substituting in the equation as follows:

$$F_{xmax} = \frac{\mu \frac{Wc}{L}}{1 + \frac{h}{L}\mu} \qquad (2\text{-}26)$$

$$F_{xmax} = \frac{(0.62)\ 1950\ \text{lb}}{1 + \frac{19}{105}\ 0.62} = \frac{1209\ \text{lb}}{1 + 0.1122} = 1087\ \text{lb}$$

$$a_x = \frac{F_{xmax}}{M\,g} = \frac{1087\ \text{lb}}{3100\ \text{lb}} = 0.3506\ \text{g's} = 11.29\ \frac{\text{ft}}{\text{sec}^2}$$

Note:

1) Even though the front-wheel-drive vehicle has a much higher percentage of its weight on the drive axle, its performance is not proportionately better. The reason is the loss of load on the front (drive) axle due to longitudinal weight transfer during acceleration.

REFERENCES

1. Gillespie, T.D., "Methods of Predicting Truck Speed Loss on Grades," The University of Michigan Transportation Research Institute, Report No. UM-85-39, November 1986, 169 p.
2. St. John, A.D., and Kobett, D.R., "Grade Effects on Traffic Flow Stability and Capacity," Interim Report, National Cooperative Highway Research Program, Project 3-19, December 1972, 173 p.
3. Marshall, H.P., "Maximum and Probable Fuel Economy of Automobiles," SAE Paper No. 800213, 1980, 8 p.

4. Cole, D., "Elementary Vehicle Dynamics," course notes in Mechanical Engineering, The University of Michigan, Ann Arbor, Michigan, 1972.
5. Smith, G.L., "Commercial Vehicle Performance and Fuel Economy," SAE Paper, SP-355, 1970, 23 p.
6. Buck, R.E., "A Computer Program (HEVSIM) for Heavy Duty Vehicle Fuel Economy and Performance Simulation," U.S. Department of Transportation, Research and Special Projects Administration, Transportation Systems Center, Report No. DOT-HS-805-912, September 1981, 26 p.
7. Zub, R.W., "A Computer Program (VEHSIM) for Vehicle Fuel Economy and Performance Simulation (Automobiles and Light Trucks)," U.S. Department of Transportation, Research and Special Projects Administration, Transportation Systems Center, Report No. DOT-HS-806-040, October 1981, 50 p.
8. Phillips, A.W., Assanis, D.N., and Badgley, P., "Development and Use of a Vehicle Powertrain Simulation for Fuel Economy and Performance Studies," SAE Paper No. 900619, 1990, 14 p.

CHAPTER 3
BRAKING PERFORMANCE

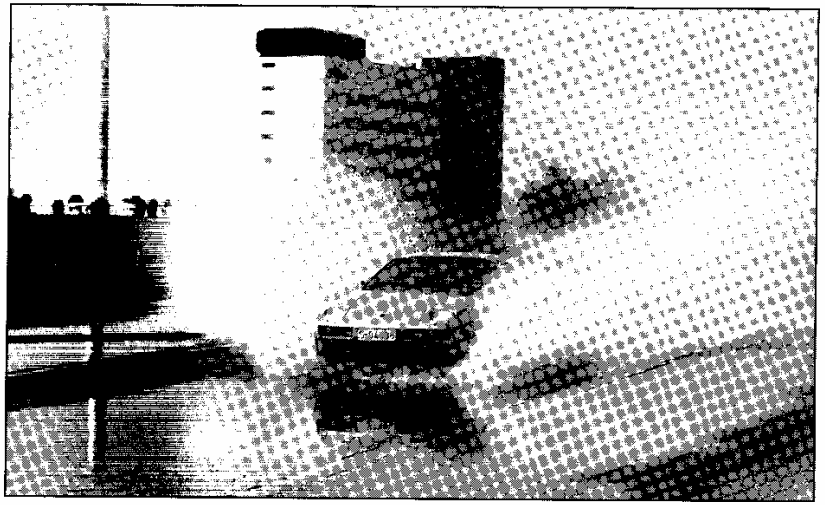

ABS test drive. (Photo courtesy of Robert Bosch GmbH.)

BASIC EQUATIONS

The general equation for braking performance may be obtained from Newton's Second Law written for the x-direction. The forces on the vehicle are generally of the type shown in Figure 1.6. Then, NSL is:

$$M a_x = -\frac{W}{g} D_x = - F_{xf} - F_{xr} - D_A - W \sin \Theta \qquad (3\text{-}1)$$

where:

W = Vehicle weight
g = Gravitational acceleration
$D_x = - a_x$ = Linear deceleration
F_{xf} = Front axle braking force
F_{xr} = Rear axle braking force
D_A = Aerodynamic drag
Θ = Uphill grade

The front and rear braking force terms arise from the torque of the brakes along with rolling resistance effects, bearing friction, and driveline drags. A comprehensive analysis of the deceleration requires detailed knowledge of all these forces acting on the vehicle.

Constant Deceleration

Simple and fundamental relationships can be derived for the case where it is reasonable to assume that the forces acting on the vehicle will be constant throughout a brake application. The simple equations that result provide an appreciation for the basic relationships that govern braking maneuvers. From Eq. (3-1):

$$D_x = \frac{F_{xt}}{M} = -\frac{dV}{dt} \tag{3-2}$$

where:

F_{xt} = The total of all longitudinal deceleration forces on the vehicle (+)

V = Forward velocity

This equation can be integrated (because F_{xt} is constant) for a deceleration (snub) from initial velocity, V_o, to final velocity, V_f:

$$\int_{V_o}^{V_f} dV = -\frac{F_{xt}}{M}\int_0^{t_s} dt \tag{3-3}$$

$$V_o - V_f = \frac{F_{xt}}{M} t_s \tag{3-4}$$

where:

t_s = Time for the velocity change

Because velocity and distance are related by V = dx/dt, we can substitute for "dt" in Eq. (3-2), integrate, and obtain the relationship between velocity and distance:

$$\frac{V_o^2}{2} - \frac{V_f^2}{2} = \frac{F_{xt}}{M} X \tag{3-5}$$

where:

X = Distance traveled during the deceleration

In the case where the deceleration is a full stop, then V_f is zero, and X is the stopping distance, SD. Then:

$$SD = \frac{V_o^2}{2\frac{F_{xt}}{M}} = \frac{V_o^2}{2 D_x} \tag{3-6}$$

and the time to stop is:

$$t_s = \frac{V_o}{\frac{F_{xt}}{M}} = \frac{V_o}{D_x} \tag{3-7}$$

Thus, all other things being equal, the time to stop is proportional to the velocity, whereas the distance is proportional to the velocity squared (i.e., doubling the velocity doubles the time to stop, but quadruples the distance required).

Deceleration with Wind Resistance

The aerodynamic drag on a vehicle is dependent on vehicle drag factors and the square of the speed. To determine stopping distance in such cases, a more complicated expression is necessary but can still be integrated. To analyze this case:

$$\Sigma F_x = F_b + C V^2 \tag{3-8}$$

where:

F_b = Total brake force of front and rear wheels

C = Aerodynamic drag factor

Therefore:

$$\int_0^{SD} dx = M \int_{V_0}^{0} \frac{V\,dV}{F_b + C V^2} \tag{3-9}$$

This may be integrated to obtain the stopping distance:

$$SD = \frac{M}{2C} \ln \left[\frac{F_b + C V_o^2}{F_b} \right] \quad (3\text{-}10)$$

Energy/Power

The energy and/or power absorbed by a brake system can be substantial during a typical maximum-effort stop. The energy absorbed is the kinetic energy of motion for the vehicle, and is thus dependent on the mass.

$$\text{Energy} = \frac{M}{2} (V_o^2 - V_f^2) \quad (3\text{-}11)$$

The power absorption will vary with the speed, being equivalent to the braking force times the speed at any instant of time. Thus, the power dissipation is greatest at the beginning of the stop when the speed is highest. Over the entire stop, the average power absorption will be the energy divided by the time to stop. Thus:

$$\text{Power} = \frac{M}{2} \frac{V_o^2}{t_s} \quad (3\text{-}12)$$

Calculation of the power is informative from the standpoint of appreciating the performance required from a brake system. A 3000 lb car in a maximum-effort stop from 80 mph requires absorption of nearly 650,000 ft-lb of energy. If stopped in 8 seconds (10 mph/sec), the average power absorption of the brakes during this interval is 145 HP. An 80,000 lb truck stopped from 60 mph typically involves dissipation at an average rate of several thousands of horsepower!

BRAKING FORCES

The forces on a vehicle producing a given braking deceleration may arise from a number of sources. Though the brakes are the primary source, others will be discussed first.

Rolling Resistance

Rolling resistance always opposes vehicle motion; hence, it aids the brakes. The rolling resistance forces will be:

$$R_{xf} + R_{xr} = f_r (W_f + W_r) = f_r W \quad (3\text{-}13)$$

The parameter "f_r" is the rolling resistance coefficient, which will be discussed in the next chapter. Note that the total force is independent of the distribution of loads on the axles (static or dynamic). Rolling resistance forces are nominally equivalent to about 0.01 g deceleration (0.3 ft/sec^2).

Aerodynamic Drag

The drag from air resistance depends on the dynamic pressure, and is thus proportional to the square of the speed. At low speeds it is negligible. At normal highway speeds, it may contribute a force equivalent to about 0.03 g (1 ft/sec^2). More discussion of this topic is presented in the next chapter.

Driveline Drag

The engine, transmission, and final drive contribute both drag and inertia effects to the braking action. As discussed in the previous chapter on Acceleration Performance, the inertia of these components adds to the effective mass of the vehicle, and warrants consideration in brake sizing on the drive wheels. The drag arises from bearing and gear friction in the transmission and differential, and engine braking. Engine braking is equivalent to the "motoring" torque (observed on a dynamometer) arising from internal friction and air pumping losses. (It is worth noting that the pumping losses disappear if the engine is driven to a speed high enough to float the valves. Thus, engine braking disappears when an engine over-revs excessively. This can be a serious problem on low-speed truck engines where valve float may occur above 4000 rpm, and has been the cause of runaway accidents on long grades.) On a manual transmission with clutch engaged during braking, the engine braking is multiplied by the gear ratio selected. Torque-converter transmissions are designed for power transfer from the engine to the driveline, but are relatively ineffective in the reverse direction; hence, engine drag does not contribute substantially to braking on vehicles so equipped.

Whether or not driveline drag aids in braking depends on the rate of deceleration. If the vehicle is slowing down faster than the driveline components would slow down under their own friction, the drive wheel brakes must pick up the extra load of decelerating the driveline during the braking maneuver. On the other hand, during low-level decelerations the driveline drag may be sufficient to decelerate the rotating driveline components and contribute to the braking effort on the drive wheels as well.

Grade

Road grade will contribute directly to the braking effort, either in a positive sense (uphill) or negative (downhill). Grade is defined as the rise over the run (vertical over horizontal distance). The additional force on the vehicle arising from grade, R_g, is given by:

$$R_g = W \sin \Theta \qquad (3\text{-}14)$$

For small angles typical of most grades:

$$\Theta \text{ (radians)} \cong \text{Grade} = \text{Rise/run}$$

$$R_g = W \sin \Theta \cong W \Theta$$

Thus a grade of 4% (0.04) will be equivalent to a deceleration of ± 0.04 g (1.3 ft/sec^2).

BRAKES

Automotive brakes in common usage today are of two types—drum and disc [1, 2, 3] as shown in Figure 3.1.

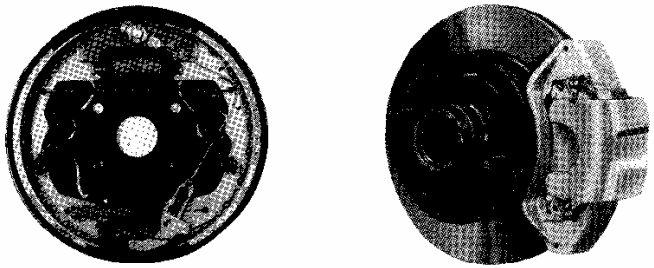

Fig. 3.1 Drum brake and disc brake. (Photo courtesy of Chrysler Corp.)

Historically, drum brakes have seen common usage in the U.S. because of their high brake factor and the easy incorporation of parking brake features. On the negative side, drum brakes may not be as consistent in torque performance as disc brakes. The lower brake factors of disc brakes require higher actuation effort, and development of integral parking brake features has been required before disc brakes could be used at all wheel positions.

Brake Factor

Brake factor is a mechanical advantage that can be utilized in drum brakes to minimize the actuation effort required. The mechanism of a common drum brake is shown in simplified form in Figure 3.2. The brake consists of two shoes pivoted at the bottom. The application of an actuation force, P_a, pushes the lining against the drum generating a friction force whose magnitude is the normal load times the coefficient of friction (μ) of the lining material against the drum. Taking moments about the pivot point for shoe A:

$$\Sigma M_p = e P_a + n \mu N_A - m N_A = 0 \qquad (3\text{-}15)$$

where:

e = Perpendicular distance from actuation force to pivot
N_A = Normal force between lining A and drum
n = Perpendicular distance from lining friction force to pivot
m = Perpendicular distance from the normal force to the pivot

The friction force developed by each brake shoe is:

$$F_A = \mu N_A \quad \text{and} \quad F_B = \mu N_B$$

Then equation (3-15) can be manipulated to obtain:

$$\frac{F_A}{P_a} = \frac{\mu e}{(m - \mu n)} \quad \text{and} \quad \frac{F_B}{P_a} = \frac{\mu e}{(m + \mu n)} \qquad (3\text{-}16)$$

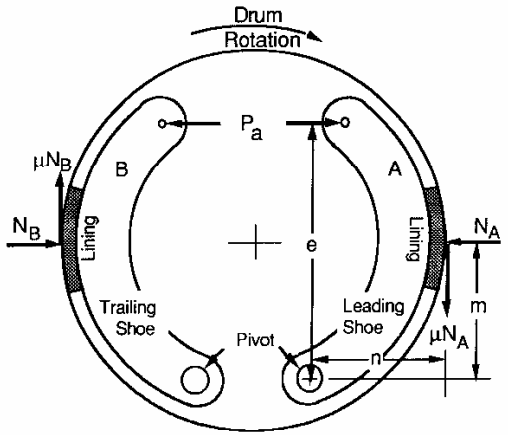

Fig. 3.2 Forces acting on the shoes of a simple drum brake.

The shoe on the right is a "leading" shoe. The moment produced by the friction force on the shoe acts to rotate it against the drum and increase the friction force developed. This "self-servo" action yields a mechanical advantage characterized as the "brake factor." The brake factor is not only proportional to μ in the numerator, but is increased by its influence in the denominator. (The expressions become more complicated with lining distributed over a larger arc, but show the same effect.) Clearly, if μ gets too large, the term "μn" may equal "m" and the brake factor goes to infinity, in which case the brake will lock on application.

Shoe B is a trailing shoe configuration on which the friction force acts to reduce the application force. The brake factor is much lower, and higher application forces are required to achieve the desired braking torque.

By using two leading shoes, two trailing shoes, or one of each, different brake factors can be obtained. The duo-servo brake has two leading shoes coupled together to obtain a very high brake factor. The consequences of using high brake factors is sensitivity to the lining coefficient of friction, and the possibility of more noise or squeal. Small changes in μ due to heating, wear, or other factors cause the brake to behave more erratically. Since disc brakes lack this self-actuation effect they generally have better torque consistency, although at the cost of requiring more actuation effort.

The difference between the two types of brakes can usually be seen in their torque properties during a stop. Brake torque performance can be measured in the laboratory using an inertial dynamometer, which is simply a large rotating mass attached to the drum with provisions to measure the torque obtained. The brake is applied with a constant actuation force to stop a rotating inertia nominally equivalent to the mass carried at the wheel on which it might be used. The torque measured during the stop typically looks like that shown in Figure 3.3.

On drum brakes, the torque will often exhibit a "sag" in the intermediate portion of the stop. It has been hypothesized that the effect is the combination of temperature fade and velocity effects (torque increases as velocity decreases). Disc brakes normally show less torque variation in the course of a stop. With an excess of these variations during a brake application, it can be difficult to maintain the proper balance between front and rear braking effort during a maximum-effort stop. Ultimately this can show up as less consistent deceleration performance in braking maneuvers resulting in longer stopping distances [6].

The torque from the brake can be modeled from the curves such as shown in Figure 3.3, but can be difficult to predict accurately over all conditions of

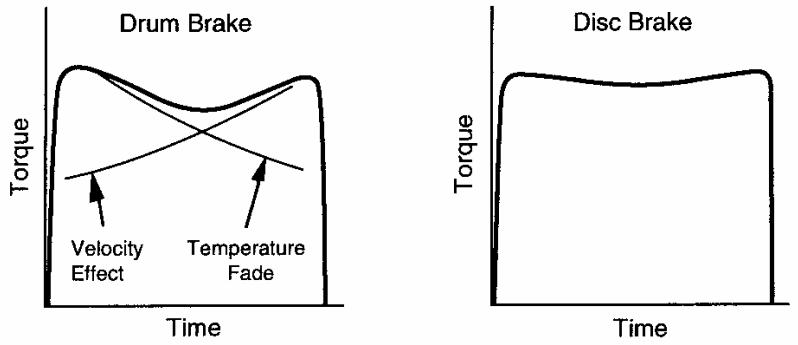

Fig. 3.3 Inertia dynamometer torque measurements.

operation. The torque normally increases almost linearly with the actuation effort, P_a, but to levels that vary with the speed and the energy absorbed (through the temperatures generated). Thus:

$$T_b = f(P_a, \text{Velocity}, \text{Temperature}) \tag{3-17}$$

Efforts to model brakes by a general equation including each of the independent factors and the interrelated effects results in a torque equation which may require up to 27 coefficients. Because the equation depends on the brake temperature, which increases during a brake application, it is necessary to incorporate a thermal model of the brake in the calculation process [11]. Experience at The University of Michigan in trying to model brake torque performance in this fashion has been only partially successful. For moderate-level applications, good predictions can be obtained. However, a high-energy application (in which the temperature gets above 650°F) will permanently change the brake such that a new set of 27 coefficients must be determined.

The torque produced by the brake acts to generate a braking force at the ground and to decelerate the wheels and driveline components. Then:

$$F_b = \frac{(T_b - I_w \alpha_w)}{r} \tag{3-18}$$

where:

r = Rolling radius of the tires
I_w = Rotational inertia of wheels (and drive components)
α_w = Rotational deceleration of wheels

Except during a wheel lockup process, α_w is related to the deceleration of the vehicle through the radius of the wheel ($\alpha_w = a_x/r$), and I_w may be simply lumped in with the vehicle mass for convenience in calculation. In that case the torque and brake force are related by the relationship:

$$F_b = \frac{T_b}{r} \tag{3-19}$$

TIRE-ROAD FRICTION

As long as all wheels are rolling, the braking forces on a vehicle can be predicted using Eq. (3-19). However, the brake force can only increase to the limit of the frictional coupling between the tire and road.

There are two primary mechanisms responsible for friction coupling as illustrated in Figure 3.4. Surface adhesion arises from the intermolecular bonds between the rubber and the aggregate in the road surface. The adhesion component is the larger of the two mechanisms on dry roads, but is reduced substantially when the road surface is contaminated with water; hence, the loss of friction on wet roads.

The bulk hysteresis mechanism represents energy loss in the rubber as it deforms when sliding over the aggregate in the road. Bulk (or hysteretic) friction is not so affected by water on the road surface, thus better wet traction is achieved with tires that have high-hysteresis rubber in the tread.

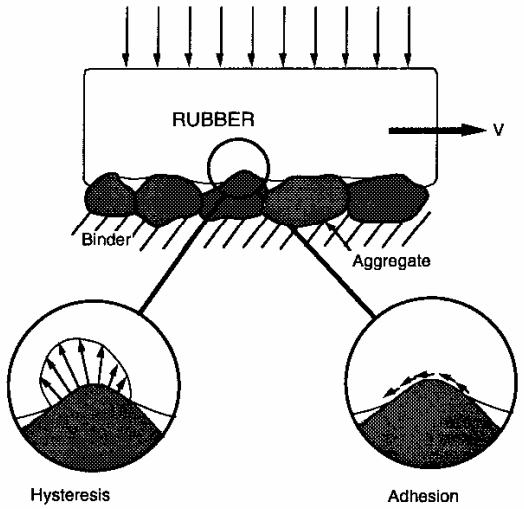

Fig. 3.4 Mechanisms of tire-road friction [4].

Both adhesive and hysteretic friction depend on some small amount of slip occurring at the tire-road interface. Additional slip is observed as a result of the deformation of the rubber elements of the tire tread as they deform to develop and sustain the braking force. This mechanism is illustrated in Figure 3.5. As the element enters the tire contact patch, it is undeformed. As it proceeds into the center of tire contact, deformation must occur for the tire to sustain a friction force. The deformation increases from the front to the back of the tire contact patch, and the force developed by each element increases proportionately from front to back. At high braking levels, the elements in the rear extreme of the contact patch begin to slide on the surface, and the braking force from the tire may begin to decrease.

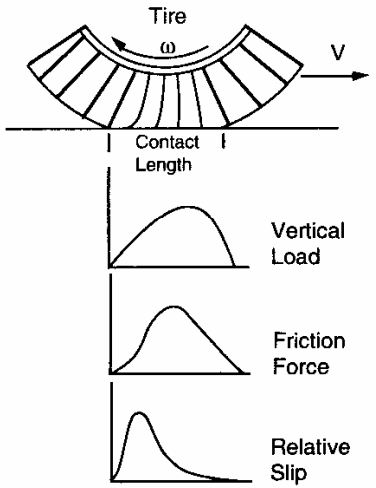

Fig 3.5 Braking deformations in the contact patch.

Because of these mechanisms, the brake force and slip are coexistent. Brake force (expressed as a coefficient F_x/F_z) is shown as a function of slip in Figure 3.6. Slip of the tire is defined by the ratio of slip velocity in the contact patch (forward velocity - tire circumferential speed) to forward velocity:

$$\text{Slip} = \frac{V - \omega r}{V} \tag{3-20}$$

where:

V = Vehicle forward velocity
ω = Tire rotational speed (radians/sec)

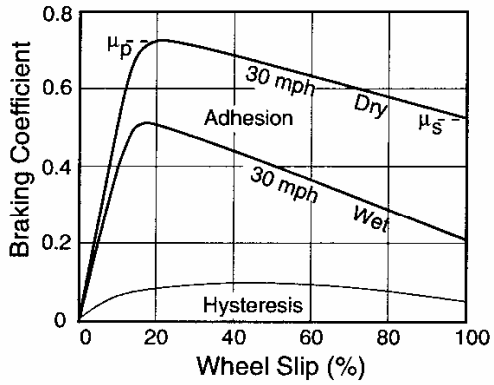

Fig. 3.6 Braking coefficient versus slip [4].

The brake coefficient deriving from adhesive and hysteretic friction increases with slip up to about 10 to 20% in magnitude depending on conditions. Under wet road conditions, the adhesive friction contribution is diminished such that the overall coefficient is lower. The peak coefficient is a key property, usually denoted by μ_p. It establishes the maximum braking force that can be obtained from the particular tire-road friction pair. At higher slip, the coefficient diminishes, reaching its lowest value at 100% slip, representing the full lock condition and denoted by μ_s. In a braking situation, μ_p corresponds to the highest brake force that can be generated, and is only theoretically possible to achieve because the system is unstable at this point. For a given brake torque output level, once the wheel is decelerated to achieve μ_p, any disturbance about this condition results in an excess of brake torque which causes further deceleration of the wheel. The increased slip reduces the brake force such that the wheel deceleration continues and the wheel goes to lock. Only a brake release (as in an anti-lock control) can return the wheel to operation at μ_p.

In addition to the tire and the road as key elements in determining the friction coupling available, other variables are important, as follows.

Velocity

On dry roads, both peak and slide friction decrease with velocity. Under wet conditions, even greater speed sensitivity prevails because of the difficulty of displacing water in the contact patch at high speeds. When the speed and water film thickness are sufficient, the tire tread will lift from the road creating a condition known as hydroplaning.

Inflation Pressure

On dry roads, peak and slide coefficients are only mildly affected by inflation pressure. On wet surfaces, inflation pressure increases are known to significantly improve both coefficients.

Vertical Load

Increasing vertical load is known to categorically reduce normalized traction levels (F_x/F_z) under both wet and dry conditions. That is, as load increases, the peak and slide friction forces do not increase proportionately. Typically, in the vicinity of a tire's rated load, both coefficients will decrease on the order of 0.01 for a 10% increase in load.

EXAMPLE PROBLEMS

1) Consider a light truck weighing 3635 lb, performing a full stop from 60 mph on a level surface with a brake application that develops a steady brake force of 2000 lb. Determine the deceleration, stopping distance, time to stop, energy dissipated and the brake horsepower at initial application and averaged over the stop. Neglect aerodynamic and rolling resistance forces.

Solution:

The deceleration may be calculated from NSL:

$$D_x = \frac{F_x}{M} = \frac{F_b}{M} = \frac{(2000\ \text{lb})\ 32.2\ \text{ft/sec}^2}{3635\ \text{lb}} = 17.72\ \frac{\text{ft}}{\text{sec}^2}$$

The deceleration can be computed directly in terms of g's by using the equational form:

$$D_x\,(g) = \frac{F_x}{W} = \frac{F_b}{W} = \frac{2000\ \text{lb}}{3635\ \text{lb}} = 0.55\ g = 12.08\ \frac{\text{mph}}{\text{sec}}$$

Now that the deceleration is known, the stopping distance may be computed (Eq. (3-6)):

$$SD = \frac{V_o^2}{2\,\frac{F_{xt}}{M}} = \frac{V_o^2}{2\,D_x} \qquad (3\text{-}6)$$

$$= \frac{(88\ \text{ft/sec})^2}{2\,(17.72\ \text{ft/sec}^2)} = 218.51\ \text{ft}$$

The time to stop comes from Eq. (3-7):

$$t_s = \frac{V_o}{F_{xt}/M} = \frac{88 \text{ ft/sec}}{17.72 \text{ ft/sec}^2} = 4.966 \text{ sec}$$

The energy dissipated comes from Eq. (3-11):

$$\text{Energy} \cong \frac{M}{2}(V_o^2 - V_f^2) = \frac{3635 \text{ lb}}{2\,(32.2 \text{ ft/sec}^2)}\,(88 \text{ ft/sec})^2$$

$$= 437{,}103 \text{ ft-lb}$$

The power dissipation at the point of brake application is simply the brake force times the forward velocity, which is:

$$\text{Power (initial)} = (2000 \text{ lb})\ 88 \text{ ft/sec} = 176{,}000 \text{ ft-lb/sec}$$

$$\text{HP (initial)} = (176{,}000 \frac{\text{ft-lb}}{\text{sec}})\ \frac{1 \text{ hp}}{550 \text{ ft-lb/sec}} = 320 \text{ hp}$$

On average over the stop, the power (from Eq. (3-12)) is:

$$\text{Power} = \frac{M}{2}\frac{V_o^2}{t_s} = \frac{3635 \text{ lb}}{2\,(32.2 \text{ ft/sec}^2)}\ \frac{(88 \text{ ft/sec})^2}{4.966 \text{ sec}}$$

$$= \frac{437{,}103 \text{ ft-lb}}{4.966 \text{ sec}} = 88{,}019 \frac{\text{ft-lb}}{\text{sec}} = 160 \text{ hp}$$

2) For the vehicle described in the previous problem, calculate the stopping distance taking aerodynamic drag into account. The aerodynamic drag force will be given by:

$$F_a = C\,V^2 = 0.00935\,(\frac{\text{lb-sec}^2}{\text{ft}^2})\ V^2\,(\frac{\text{ft}^2}{\text{sec}^2})$$

The stopping distance may be computed from Eq. (3-10):

$$SD = \frac{M}{2C}\ln[\frac{(F_b + C\,V_o^2)}{F_b}] \qquad (3\text{-}10)$$

$$= \frac{3635 \text{ lb}}{2\,(0.00935 \frac{\text{lb-sec}^2}{\text{ft}^2})\,(32.2 \frac{\text{ft}}{\text{sec}^2})}\ln\frac{2000 \text{ lb} + 0.00935 \frac{\text{lb-sec}^2}{\text{ft}^2}(88 \frac{\text{ft}}{\text{sec}})^2}{2000 \text{ lb}}$$

$$= 214.69 \text{ ft}$$

Thus, roughly 4 feet will be cut from the stopping distance when aerodynamic drag is included in the calculation. The drag itself is only 74.4 lb at the beginning of the stop and decreases with the square of the velocity, so its contribution becomes much less during the course of the stop.

FEDERAL REQUIREMENTS FOR BRAKING PERFORMANCE

Out of the public concern for automotive safety in the 1960s, the Highway Safety Act of 1965 was passed establishing the National Highway Traffic Safety Administration charged with promulgating performance standards for new vehicles which would increase safety on the highways. Among the many standards that have been imposed are Federal Motor Vehicle Safety Standard (FMVSS) 105 [5], establishing braking performance requirements for vehicles with hydraulic brake systems, and FMVSS 121 [6], establishing braking performance requirements for vehicles with air brake systems.

FMVSS 105 defines service brake and parking brake performance requirements over a broad range of conditions, such as:

- Lightly loaded to fully loaded at gross vehicle weight rating (GVWR)
- Preburnish to full burnish conditions
- Speeds from 30 to 100 mph
- Partially failed systems tests
- Failure indicator systems
- Water recovery
- Fade and recovery
- Brake control force limits

Although the standard is quite detailed and complex, the requirements for stopping distance performance can be summarized into five tests:

1) First effectiveness—A fully loaded passenger car with new, unburnished brakes must be able to stop from speeds of 30 and 60 mph in distances that correspond to average decelerations of 17 and 18 ft/sec^2, respectively.

2) Second effectiveness—A fully loaded passenger car with burnished[1] brakes must be able to stop from 30, 60 and 80 mph in distances that correspond to average decelerations of 17, 19 and 18 ft/sec^2, respectively.

3) Third effectiveness—A lightly loaded passenger car with burnished brakes must be able to stop from 60 mph in a distance that corresponds to an average deceleration of 20 ft/sec^2.

4) Fourth effectiveness—A fully loaded passenger car with burnished brakes must be able to stop from 30, 60, 80 and 100 mph in distances that correspond to average decelerations of 17, 18, 17 and 16 ft/sec^2, respectively.

5) Partial failure—A lightly loaded and fully loaded passenger car with a failure in the brake system must be able to stop from 60 mph in a distance that corresponds to an average deceleration of 8.5 ft/sec^2.

It is notable that the hydraulic brake standard (FMVSS 105) has stopping distance requirements only for dry surfaces of an 81 Skid Number. (Skid Number is the tire-road friction coefficient measured by American Society for Testing and Materials Method E-274-85 [8]. Although the Skid Number is measured with a special, standard tire, the Skid Number and coefficient of friction are generally assumed to be equivalent.) The air brake vehicle standard (FMVSS 121) has stopping distance performance requirements on both wet surfaces (30 Skid Number) and dry surfaces (81 Skid Number). Obviously, the prudent brake system designer considers a range of surface friction conditions, from at least 30 to 81 SN, despite any gaps in the Federal performance standards.

BRAKE PROPORTIONING

The braking decelerations achievable on a vehicle are simply the product of application level and the brake gains (torque/pressure) up to the point where lockup will occur on one of the axles. Lockup reduces the brake force on an axle, and results in some loss of ability to control the vehicle. It is well recognized that the preferred design is to bring both axles up to the lockup point simultaneously. Yet, this is not possible over the complete range of operating conditions to which a vehicle will be exposed. Balancing the brake outputs on both the front and rear axles is achieved by "proportioning" the pressure

[1] Burnish refers to a process in which new brakes are "worn in" by repeated brake applications according to a procedure defined in the standard.

appropriately for the foundation brakes installed on the vehicle. Proportioning then adjusts the brake torque output at front and rear wheels in accordance with the peak traction forces possible.

The first-order determinants of peak traction force on an axle are the instantaneous load and the peak coefficient of friction. During braking, a dynamic load transfer from the rear to the front axle occurs such that the load on an axle is the static plus the dynamic load transfer contributions. Thus for a deceleration, D_x:

$$W_f = \frac{c}{L} W + \frac{h}{L} \frac{W}{g} D_x = W_{fs} + W_d \tag{3-21}$$

and

$$W_r = \frac{b}{L} W - \frac{h}{L} \frac{W}{g} D_x = W_{rs} - W_d \tag{3-22}$$

where:

W_{fs} = Front axle static load

W_{rs} = Rear axle static load

$W_d = (h/L)\,(W/g)\,D_x$ = Dynamic load transfer

Then, on each axle the maximum brake force is given by:

$$F_{xmf} = \mu_p W_f = \mu_p \left(W_{fs} + \frac{h}{L} \frac{W}{g} D_x\right) \tag{3-23}$$

and

$$F_{xmr} = \mu_p W_r = \mu_p \left(W_{rs} - \frac{h}{L} \frac{W}{g} D_x\right) \tag{3-24}$$

where:

μ_p = Peak coefficient of friction

The maximum brake force is dependent on the deceleration, varying differently at each axle. Figure 3.7 shows graphically the maximum brake forces according to the above equations for a typical passenger car on both a high and low coefficient surface. The deceleration is shown in units of g's (equivalent to D/g). Attempts at braking on an axle above the boundary value results in lockup on the axle.

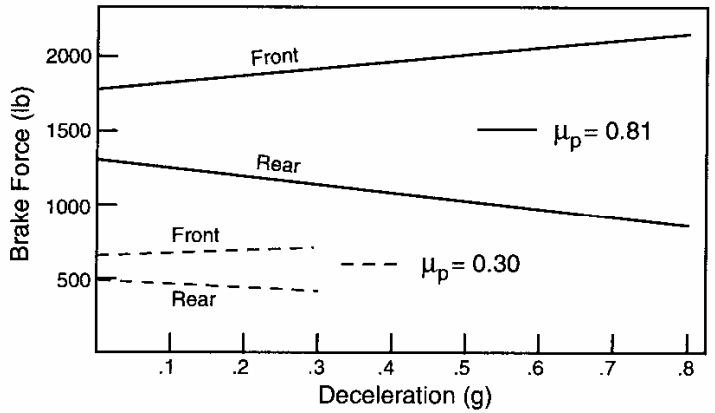

Fig. 3.7 Maximum brake forces as a function of deceleration.

Inasmuch as the equations above contain the deceleration as a variable, they do not provide an explicit solution for the maximum braking forces on an axle. These can be obtained by recognizing that the deceleration is a function of the total braking force imposed on the vehicle (neglecting for simplicity the other forces that may be present). To solve for F_{xmf}, we can use the relationship:

$$D_x = \frac{(F_{xmf} + F_{xr})}{M} \tag{3-25}$$

and for F_{xmr}:

$$D_x = \frac{(F_{xmr} + F_{xf})}{M} \tag{3-26}$$

Substituting into Eqs. (3-23) and (3-24) yields the following equations for the maximum braking force on each axle:

$$F_{xmf} = \frac{\mu_p (W_{fs} + \frac{h}{L} F_{xr})}{1 - \mu_p \frac{h}{L}} \tag{3-27}$$

$$F_{xmr} = \frac{\mu_p (W_{rs} - \frac{h}{L} F_{xf})}{1 + \mu_p \frac{h}{L}} \tag{3-28}$$

Thus the maximum braking force on the front axle is dependent on that present on the rear axle through the deceleration and associated forward load transfer resulting from the rear brake action. Conversely, the same effect is evident on the rear axle. These relationships can best be visualized by plotting the rear versus front brake forces as shown in Figure 3.8.

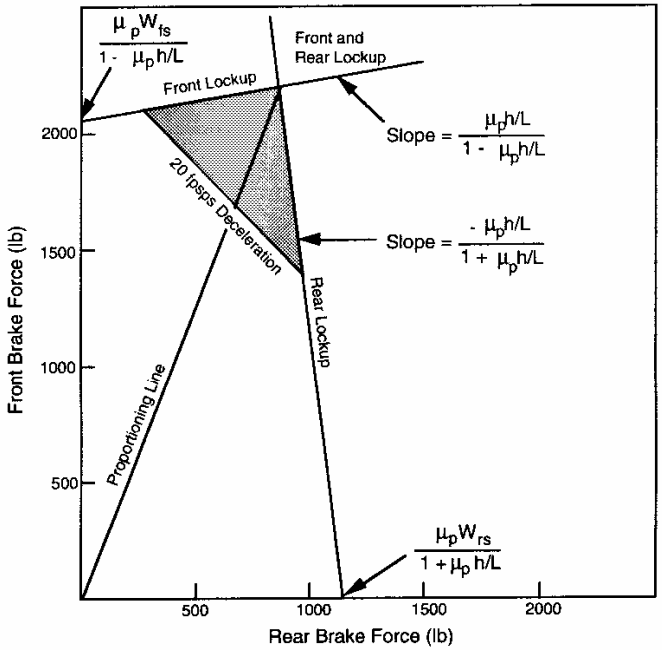

Fig. 3.8 Maximum braking forces on the front and rear axles.

The horizontal axis represents rear brake force, which is generally proportional to the rear brake pressure (related by the torque-to-pressure relationship for that foundation brake). The vertical axis is front brake force, again proportional to front brake pressure in accordance with the brake gain. The origin of each line is obtained from Eqs. (3-27) and (3-28) by setting the brake force of the opposite brake to zero.

Lines for the maximum front axle brake force slope upward and to the right (positive) at the slope of μ_p h/L /(1- μ_p h/L). Lines for the rear axle maximum brake force slope downward to the right (negative) with a slope that is equal to - μ_p h/L /(1+ μ_p h/L). Increasing the surface coefficient or the CG height

increases the slopes of the maximum brake force lines on the graph. Varying the load condition on the vehicle translates the origin of each of the lines on the graph. The intersection point for the front and rear brake boundaries can be determined by manipulating equations (3-27) and (3-28). Designating the points as F_{xfi} and F_{xri}, it can be shown that these coordinates are:

$$F_{xfi} = \mu \left(W_{fs} + \mu W \frac{h}{L}\right) \tag{3-29}$$

$$F_{xri} = \mu \left(W_{rs} - \mu W \frac{h}{L}\right) \tag{3-30}$$

An attempt to brake the vehicle to a level that goes above the front brake force boundary will cause front wheel lockup to occur, and steering control will be lost. Likewise, braking effort that falls to the right of the rear brake boundary causes rear wheel lockup, which places the vehicle in an unstable condition. The instability has safety implications and therefore warrants careful consideration in the design of the brake system. This issue is discussed in more detail in a later section.

In a graph of the form of Figure 3.8, the deceleration is proportional to the sum of the front and rear brake forces. Thus 2000 lb of front brake force with zero rear force, 1000 lb front with 1000 lb rear, and zero front with 2000 lb rear brake force, all correspond to the same deceleration level, and a line of constant deceleration can be plotted by connecting these points. If the same scale is used for the front and rear brake forces, lines of constant deceleration plot as 45-degree diagonals on the graph.

If a deceleration capability of 20 ft/sec^2 is required on the 0.81 μ surface, any combination of front to rear brake force would satisfy that requirement so long as it falls in the triangle bounded by the deceleration line and the maximum brake force lines for the 0.81 μ surface.

"Brake proportioning" describes the relationship between front and rear brake forces determined by the pressure applied to each brake and the gain of each. It is represented by a line on the graph starting at the origin and extending upward and to the right. A fixed, or constant, proportioning is a straight line.

The primary challenge in brake system design is the task of selecting a proportioning ratio (the slope of a line on the graph) that will satisfy all design goals despite the variabilities in surface friction, front/rear weight distribution, CG height, and brake condition. A number of these objectives are defined by the FMVSS 105 braking standard in the various effectiveness tests, although

performance objectives for low coefficient surfaces should be included by the brake designer as well. To date, low coefficient performance has only been specified in FMVSS 121, which defines braking performance requirements for air-braked trucks.

The primary factor determining brake proportioning is the gain of the brakes used on the front and rear wheels. The brake force on individual wheels can be described by the equation:

$$F_b = \frac{T_b}{r} = G \frac{P_a}{r} \tag{3-31}$$

where:

F_b = Brake force

T_b = Brake torque

r = Tire rolling radius

G = Brake gain (in-lb/psi)

P_a = Application pressure

Achieving good performance over the full range of conditions under which a vehicle operates can be difficult. As an example of the complexity that can be experienced in trying to identify appropriate brake proportioning, consider the case shown in Figure 3.9. The figure illustrates the range of variations that arise from vehicle loading (lightly loaded and GVWR) and surface friction (30 and 81 SN). On the graph the brake force boundaries and deceleration requirements have been plotted for the FMVSS 105 dry surface tests conditions. In addition, similar boundaries have been plotted for wet road conditions assuming a friction coefficient of 30 SN. Under the wet conditions, a deceleration performance goal of 8 ft/sec^2 (0.25 g) has been assumed.

To achieve all performance goals, a proportioning design must be selected that passes through all of the triangles shown. This cannot be achieved with a straight line providing a constant relationship between front and rear brake force. A solution to this problem is to incorporate a valve in the hydraulic system that changes the pressure going to the rear brakes over some portion of the operating pressure range. Such a valve is known as a pressure proportioning valve. Most pressure proportioning valves in common use today provide equal pressure to both front and rear brakes up to a certain pressure level, and then

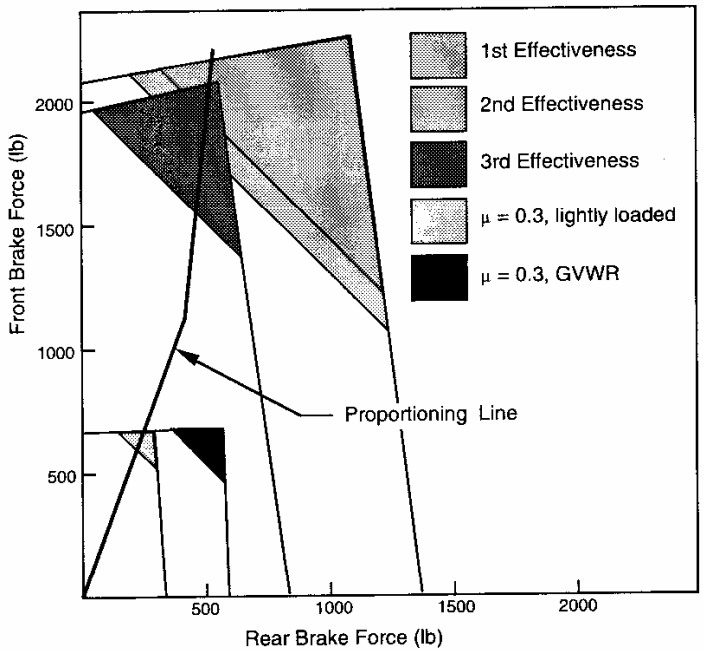

Fig. 3.9 Front/rear brake force graph for multiple braking conditions.

reduce the rate of pressure increase to one of the brakes thereafter. A proportioning valve identified as a "500/0.3" means that the pressure to the front and rear brakes is equal up to 500 psi. Above this level the pressure proportioned to the rear brakes increases at only 30% of the rate going to the front brakes. That is:

$$P_f = P_r = P_a = \text{Application pressure} \qquad \text{for } P_a < 500 \text{ psi} \qquad (3\text{-}32a)$$

$$P_f = P_a \quad \text{and} \quad P_r = 500 + 0.3\,(P_a - 500) \qquad \text{for } P_a > 500 \text{ psi} \qquad (3\text{-}32b)$$

With this proportioning it is seen that it is possible to achieve a front/rear brake balance satisfying all dry surface conditions as evidenced by the fact that the proportioning line passes through all of the performance triangles. The only exception is the fully loaded vehicle (GVWR) on the low coefficient surface, where the brake proportioning will not quite achieve 0.25 g. In every case, the plot indicates that front lockup will occur first.

Achieving good proportioning is especially difficult on trucks because of the disparity between loaded and empty conditions. Typically, the perfor-

mance triangles do not overlap in those cases, so no choice of proportioning will satisfy all goals. Several solutions are available. In Europe, load-sensing proportioning valves have been used on trucks for some years. These valves, installed on the axle(s), sense the load condition and adjust the brake proportioning appropriately. Less commonly used is the inertia-proportioning valve which senses the deceleration rate and can adjust proportioning in accordance with the deceleration level. Finally, anti-lock brake systems offer a versatile method of automatically proportioning brakes that is becoming well accepted in the automotive industry.

ANTI-LOCK BRAKE SYSTEMS

Rather than attempt to adjust the proportioning directly, anti-lock systems (ABS) sense when wheel lockup occurs, release the brakes momentarily on locked wheels, and reapply them when the wheel spins up again. Modern anti-lock brake systems are capable of releasing the brakes before the wheel goes to lockup, and modulating the level of pressure on reapplication to just hold the wheel near peak slip conditions.

The concept of ABS dates back to the 1930s, but has only become truly practical with electronics available on modern vehicles. An ABS consists of an electronic control unit (ECU), a solenoid for releasing and reapplying pressure to a brake, and a wheel speed sensor. The ECU normally monitors vehicle speed through the wheel speed sensors, and upon brake application begins to compute an estimate of the diminishing speed of the vehicle. Actual wheel speeds can be compared against the computed speed to determine whether a wheel is slipping excessively, or the deceleration rate of a wheel can be monitored to determine when the wheel is advancing toward lockup. Different ABS designs use different combinations of these variables to determine when lockup is imminent and brake release is warranted. At that point a command signal is sent to the solenoid to release the brake pressure, allowing the wheel to spin back up. Once the wheel regains speed, the pressure is increased again. Depending on the refinement of the control algorithms, the pressure rise rate and the final pressure may be controlled to minimize cycling of the brakes.

Figure 3.10 shows a typical plot of wheel speed cycling during the stop of a vehicle with ABS. When the brakes are first applied, wheel speeds diminish more or less in accordance with the vehicle speed in region 1 in the plot. If the brakes are applied to a high level, or the road is slippery, the speed of one or

more wheels begins to drop rapidly (point 2), indicating that the tire has gone through the peak of the μ-slip curve and is heading toward lockup. At this point the ABS intervenes and releases the brakes on those wheels before lockup occurs (point 3). Once the wheel speed picks up again the brakes are reapplied. The objective of the ABS is to keep each tire on the vehicle operating near the peak of the μ-slip curve for that tire. This is illustrated in Figure 3.11.

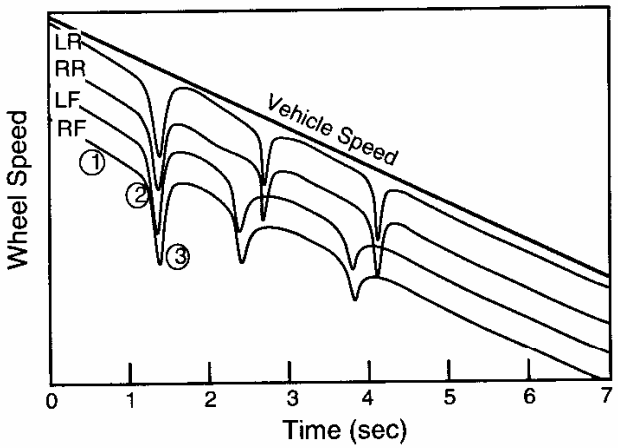

Fig. 3.10 Wheel speed cycling during ABS operation.

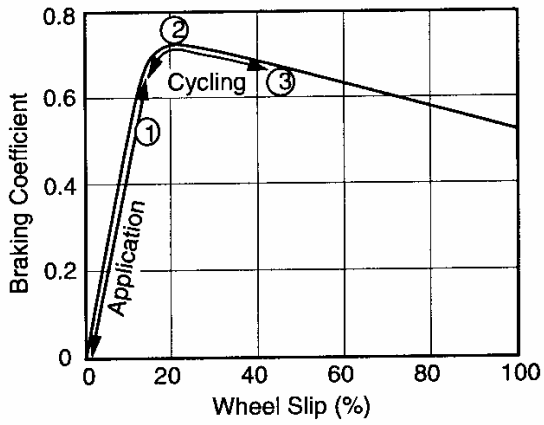

Fig 3.11 ABS operation to stay at the peak braking coefficient.

BRAKING EFFICIENCY

Recognizing that braking performance of any vehicle will vary according to the friction of the road surface on which it is attempted, the concept of braking efficiency has been developed as a measure of performance. Braking efficiency, η_b, may be defined as the ratio of actual deceleration achieved to the "best" performance possible on the given road surface. It can be shown with the use of the equations presented earlier that the best performance any vehicle can achieve is a braking deceleration (in g's) equivalent to coefficient of friction between the tires and the road surface. That is:

$$\eta_b = \frac{D_{act}}{\mu_p} \tag{3-33}$$

The braking efficiency concept is useful as a design tool for the designer to assess success in optimizing the vehicle braking system [7]. Yet implementation of braking standards using the braking efficiency approach (to avoid the problems of designating surfaces with standard friction levels via the ASTM Skid Number [8]) has been unsuccessful. The main problem has been the difficulty of defining an effective friction level for a tire-road surface pair because of the variations in friction with velocity, wheel load, tire type and other factors.

Braking efficiency is determined by calculating the brake forces, deceleration, axle loads, and braking coefficient on each axle as a function of application pressure. The braking coefficient is defined as the ratio of brake force to load on a wheel or axle. The braking efficiency at any level of application pressure is the deceleration divided by the highest braking coefficient of any axle. Since the axle with the highest braking coefficient defines the required level of road friction, the braking efficiency is also equal to the ratio of deceleration to the required road surface coefficient.

Braking efficiency is a useful method for evaluating the performance of brake systems, especially on heavy trucks where multiple axles are involved. Figure 3.12 shows the braking efficiency calculated for a five-axle tractor-semitrailer.

Contributions to braking from individual axles are better assessed by examining the braking coefficient developed on each. A plot of these curves (sometimes known as a friction utilization plot) is shown in Figure 3.13. Five curves representing the five axles of the combination are shown. Brake coefficient is defined for an axle as the ratio of brake force to load. Ideally, all

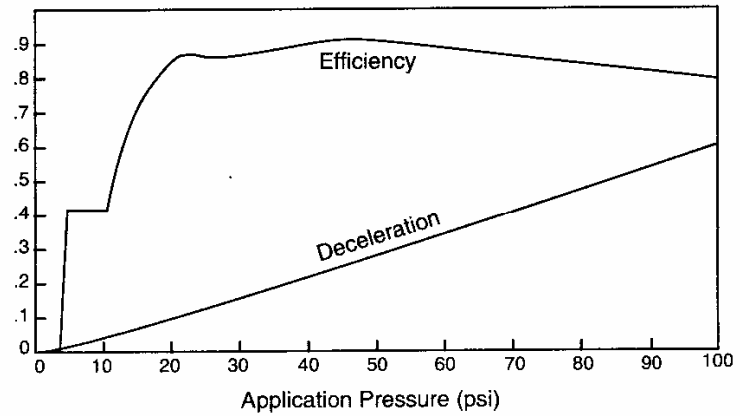

Fig 3.12 Efficiency plot for a tractor-semitrailer.

axles would have the same braking coefficient at a given application pressure, indicating that they all brake in proportion to their load. However, the diverse load conditions, longitudinal load transfer during braking, and shift of load between tandem axles due to brake reactions (inter-axle load transfer) preclude perfect harmony of the system. This is the reason the braking efficiency falls below the maximum theoretical value of 1. In the case of the tractor-semitrailer shown here, the braking efficiency rises quickly to a value of 0.9 at low brake application pressures, but drops off again at higher pressure due to the spread in braking coefficient among the axles at high deceleration conditions.

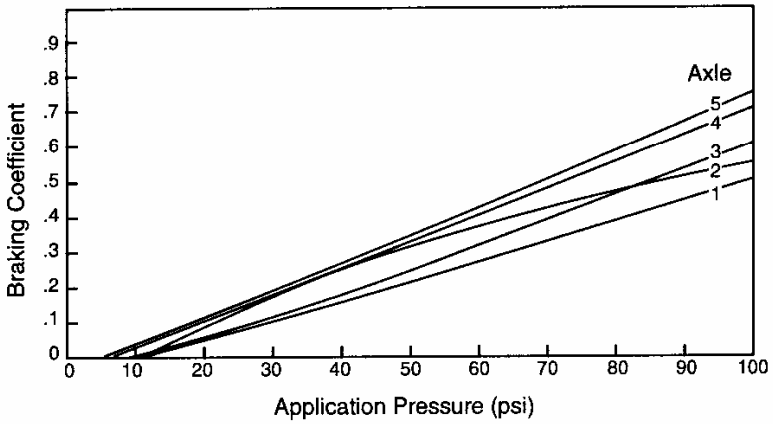

Fig 3.13 Braking coefficient on five axles of a tractor-semitrailer.

REAR WHEEL LOCKUP

In the discussion so far, wheel lockup has been considered only as a boundary on braking performance. However, it has great impact on the handling behavior of the vehicle as well, and must be considered by the brake designer. Once a wheel locks up it loses its ability to generate the cornering forces needed to keep the vehicle oriented on the road.

Lockup of front wheels causes loss of the ability to steer the vehicle, and it will generally continue straight ahead despite any steering inputs, drifting to the side only in response to cross-slope or side winds.

It is well recognized that rear wheel lockup places a motor vehicle in an unstable condition. Once the wheels lock up, any yaw disturbances (which are always present) will initiate a rotation of the vehicle. The front wheels, which yaw with the vehicle, develop a cornering force favoring the rotation, and the yaw angle continues to grow. Only when the vehicle has completely "switched ends" is it again stable. On long vehicles (some trucks and buses) the rotational accelerations are usually slow enough that the driver can apply corrective steer and prevent the full rotation. However, on smaller passenger cars, it is generally accepted that the average driver cannot readily control the vehicle in such a driving situation. Thus there is a philosophy among automotive designers that a front brake bias constitutes the preferred design.

The preference for a front brake lockup first cannot easily be achieved in a brake system design under all circumstances because of in-use variations in brake gain, CG height (particularly on light trucks), pavement friction, and parking brake requirements. The potential consequences in the hands of the motorist have been estimated using the braking efficiency as the measure of performance [9]. The basis for it arises from studies of driver behavior that show that brake applications occur on the average about 1.5 times per mile. Though most of the brake applications are executed at a moderate level, high decelerations are required in a certain percentage of the brake applications. Braking level demands of motorists are shown in Figure 3.14, which plots the percent of decelerations exceeding given deceleration levels. Twenty percent of all brake applications exceed 0.2 g, only 1% exceed 0.35 g, and less than 0.1% go up to 0.5 g.

The comparison of deceleration demands in normal driving to the available friction level of roads is shown in Figure 3.15. The distribution of road friction coefficients is estimated from numerous surveys of "skid resistance" routinely made by many highway departments. By and large, most roads have friction levels sufficient to accommodate the deceleration demands of the motorists if

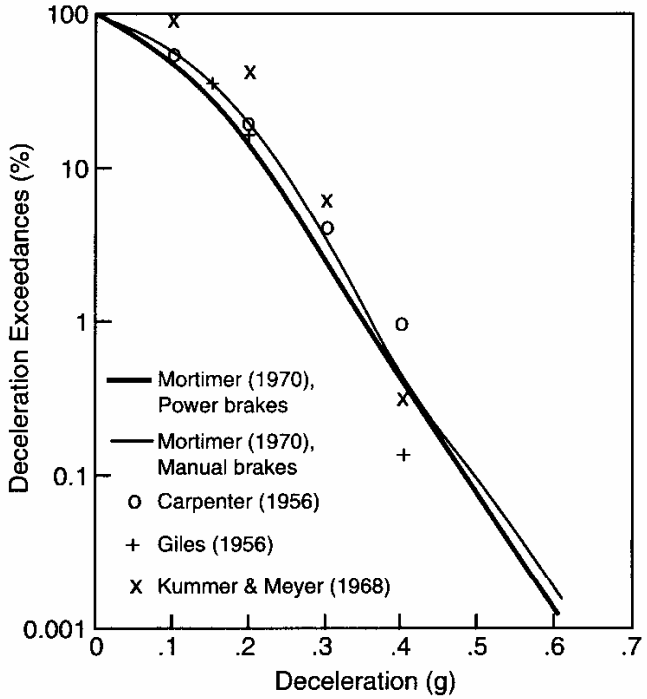

Fig. 3.14 Distribution of braking decelerations with passenger cars.

the friction is efficiently utilized. That is, if the brake systems on all vehicles were 100% efficient under all conditions, little overlap would occur in the braking "demand" and friction "available" curves, and there would be few braking instances in which wheel lockup occurs.

However, when braking efficiency is less than 100%, higher friction is required to achieve a desired deceleration level. With lower efficiency the "friction demand" curve shifts to the right. Thus the overlap and frequency at which braking demand will exceed the friction available will increase. Using the average figure of 1.5 brake applications per mile and 10,000 miles per year for a typical passenger car, the frequency of wheel lockup in braking can be estimated for different braking system efficiencies as shown in Figure 3.16. Clearly, it illustrates the acute sensitivity of lockup frequency to braking efficiency. If the inefficiency is due to a rear bias in the brake force distribution, the lockups will occur on the rear axle, and directional instability will result. Most occurrences will be on roads with lower friction levels, which are

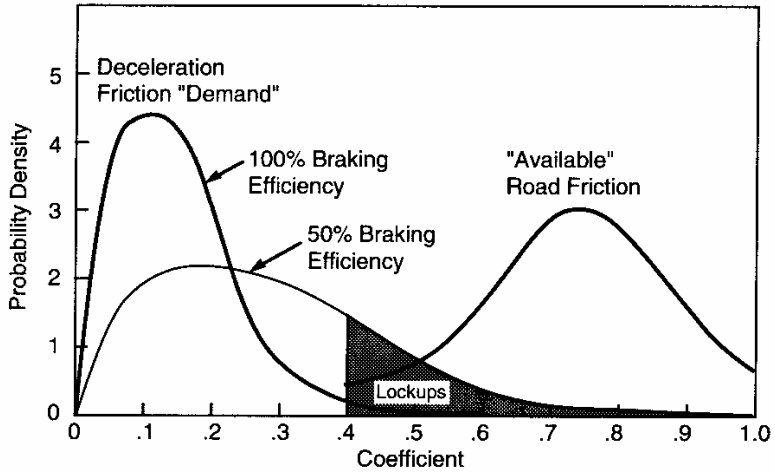

Fig. 3.15 Comparison of friction demand and availability.

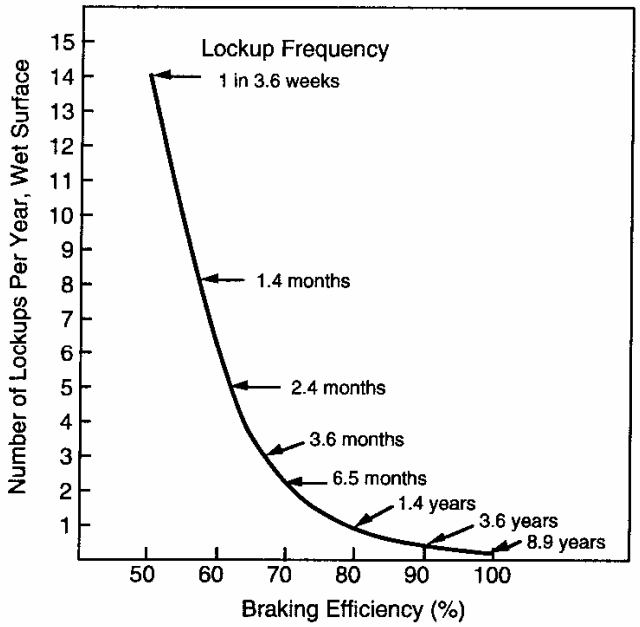

Fig. 3.16 Predicted frequency of lockup events.

normally wet road conditions. Since the majority of these instances will occur on roads with friction coefficients in the range of 0.4 to 0.6, particular emphasis should be placed on obtaining good braking system efficiency in this road friction range.

PEDAL FORCE GAIN

Ergonomics in the design of a brake system can play an important role in the ease with which the driving public can optimally use the braking capabilities built into a vehicle. Aside from positioning of the brake pedal, the effort and displacement properties of the pedal during braking are recognized as influential design variables. In the 1950s when power brake systems first came into general use, there was little uniformity among manufacturers in the level of effort and pedal displacement properties of the systems. In 1970 the National Highway Traffic Safety Administration sponsored research to determine ergonomic properties for the brake pedal that would give drivers the most effective control [10]. The research identified an optimum range for pedal force gain—the relationship between pedal force and deceleration. Figure 3.17 shows the results from the NHTSA study indicating the optimal gain values by the shaded area.

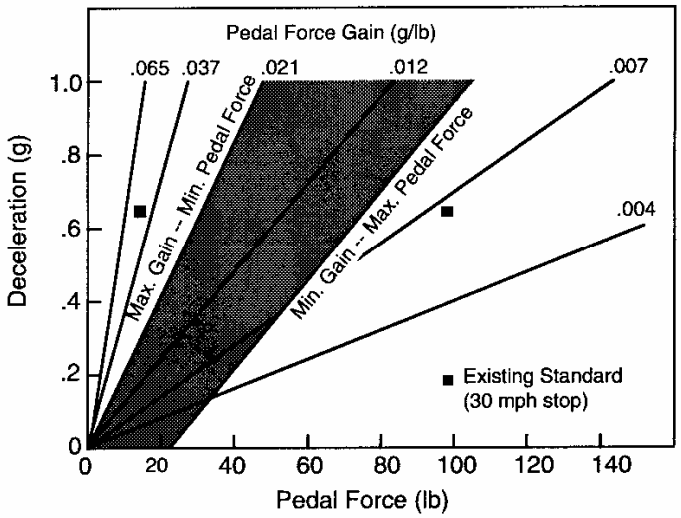

Fig. 3.17 Optimal pedal force gain properties.

EXAMPLE PROBLEM

Calculate the braking coefficients and braking efficiency for a passenger car in 100 psi increments of application pressure up to 700 psi, given the following information:

Wheelbase = 108.5 in CGH = 20.5 in Tire radius = 12.11 in

Weights: W_f = 2210 lb W_r = 1864 lb Total = 4074 lb

Front brake gain = 20 in-lb/psi Rear brake gain = 14 in-lb/psi

Proportioning valve design = 290/0.3

Solution:

The easiest way to visualize the answer is to tabulate data in columns as shown below. The calculation steps are the following:

1) The front application pressure is the reference, so we list values from 100 and up.

2) The rear application pressure is calculated from the front using the relationship similar to that given in Eq. (3-32). Namely,

$$P_r = P_a \qquad \text{for } P_a < 290 \text{ psi} \qquad (3\text{-}32a)$$

$$P_r = 290 + 0.3\,(P_a - 290) \qquad \text{for } P_a > 290 \text{ psi} \qquad (3\text{-}32b)$$

3) The front and rear brake forces are the product of the application pressure on that brake times the torque gain times two brakes per axle divided by tire radius.

$$F_{xf} = 2\,G_f \frac{P_f}{r} \qquad \text{and} \qquad F_{xr} = 2\,G_r \frac{P_r}{r}$$

4) The deceleration is the sum of the brake forces divided by total vehicle weight (this results in deceleration in units of g).

$$D_x = \frac{F_{xf} + F_{xr}}{W}$$

5) The front and rear axle loads are calculated from Eqs. (3-21) and (3-22).

$$W_f = W_{fs} + (h/L)\,(W/g)\,D_x \qquad (3\text{-}21)$$

and

$$W_r = W_{rs} - (h/L)\,(W/g)\,D_x \qquad (3\text{-}22)$$

where "D_x" is in units of ft/sec^2.

6) The braking coefficients (μ_f and μ_r) are the ratio of axle brake force to axle load.

$$\mu_f = \frac{F_{xf}}{W_f} \qquad \text{and} \qquad \mu_r = \frac{F_{xr}}{W_r}$$

7) The braking efficiency, η_b, is the deceleration divided by the highest of the two braking coefficients from the axles.

P_f	P_r	F_f	F_r	D_x	W_f	W_r	μ_f	μ_r	η_b
100 psi	100 psi	330 lb	231 lb	.138 g	2316 lb	1758 lb	.142	.131	97%
200	200	661	462	.276	2422	1652	.273	.280	99
300	293	991	677	.409	2525	1549	.393	.437	94
400	323	1321	747	.508	2601	1473	.508	.507	100
500	353	1651	816	.606	2676	1398	.617	.583	98
600	383	1982	886	.704	2752	1322	.720	.670	98
700	413	2312	955	.802	2827	1247	.818	.766	98

Notes:

a) The braking efficiency starts high (97 - 99%) by the match of the brake gains and axle loads, but begins to diminish with deceleration because of the decreasing load on the rear axle.

b) When the application pressure reaches 290 psi, the proportioning valve "kicks in" reducing the pressure rise rate on the rear axle. This brings things back into balance providing 100% efficiency at 400 psi.

REFERENCES

1. Newcomb, T.P., and Spurr, R.T., Braking of Road Vehicles, Chapman and Hall, Ltd., London, England, 1967, 292 p.
2. Limpert, R., "Analysis and Design of Motor Vehicle Brake Systems," The University of Michigan, May 1971, 466 p.
3. Engineering Design Handbook, Analysis and Design of Automotive Brake Systems, DARCOM-P 706-358, US Army Material Development and Readiness Command, Alexandria, VA, December 1976, 252 p.
4. Meyer, W.E., and Kummer, H.W., "Mechanism of Force Transmission between Tire and Road," Society of Automotive Engineers, Paper No. 620407 (490A), 1962, 18 p.
5. "Standard No. 105; Hydraulic Brake Systems," Code of Federal Regulations, Title 49, Part 571.105, October 1, 1990, pp. 199-215.
6. "Standard No. 121; Air Brake Systems," Code of Federal Regulations, Title 49, Part 571.121, October 1, 1990, pp. 366-382.
7. Gillespie, T.D., and Balderas, L., "An Analytical Comparison of a European Heavy Vehicle and a Generic U.S. Heavy Vehicle," The University of Michigan Transportation Research Institute, Report No. UMTRI-87-17, August 1987, 374 p.
8. "Test Method for Skid Resistance of Paved Surfaces Using a Full-Scale Tire," Method E274-85, 1986 Annual Book of ASTM Standards, American Society for Testing and Materials, Philadelphia, PA.
9. Ervin, R.D., and Winkler, C.B., "Estimation of the Probability of Wheel Lockup," IAVD Congress on Vehicle Design and Components, Geneva, March 3-5, 1986, pp. D145-D165.
10. Mortimer, R.E., Segel, L., Dugoff, H., Campbell, J.O., Jorgeson, C.M., and Murphy, R.W., "Brake Force Requirement Study: Driver-Vehicle Braking Performance as a Function of Brake System Design Variables," The University of Michigan Highway Safety Research Institute, Report No. HuF-6, April 1979, 22 p.
11. Johnson, L., Fancher, P.S., and Gillespie, T.D., "An Empirical Model for the Prediction of the Torque Output of Commercial Vehicle Air Brakes," Highway Safety Research Institute, University of Michigan, Report No. UM-HSRI-78-53, December 1978, 83 p.

CHAPTER 4
ROAD LOADS

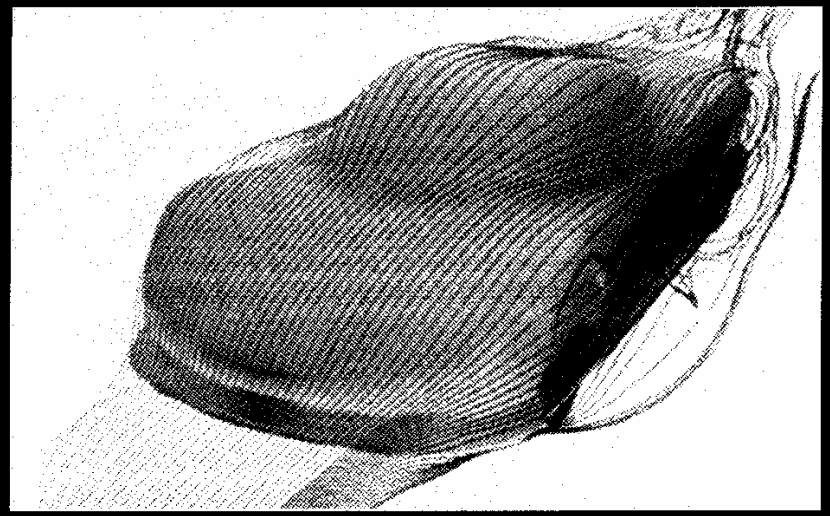

Flow field around the HSR II. (SAE Paper No. 910597.)

AERODYNAMICS

Aerodynamics makes its major impact on modern cars and trucks through its contribution to "road load." Aerodynamic forces interact with the vehicle causing drag, lift (or down load), lateral forces, moments in roll, pitch and yaw, and noise. These impact fuel economy, handling and NVH.

The aerodynamic forces produced on a vehicle arise from two sources—form (or pressure) drag and viscous friction. First, the mechanics of air flow will be examined to explain the nature of the flow around the body of the vehicle. Then, vehicle design features will be examined to show the qualitative influence on aerodynamic performance.

Mechanics of Air Flow Around a Vehicle

The gross flow over the body of a car is governed by the relationship between velocity and pressure expressed in Bernoulli's Equation [1,2].

(Bernoulli's Equation assumes incompressible flow, which is reasonable for automotive aerodynamics, whereas the equivalent relationship for compressible flow is the Euler Equation.) The equation is:

$$P_{static} + P_{dynamic} = P_{total} \qquad (4\text{-}1)$$

$$P_s + 1/2\,\rho\,V^2 = P_t$$

where:

ρ = Density of air

V = Velocity of air (relative to the car)

This relationship is derived by applying Newton's Second Law to an incremental body of fluid flowing in a well-behaved fashion. For purposes of explanation, "well-behaved" simply means that the flow is moving smoothly and is experiencing negligible friction—conditions that apply reasonably to the air stream approaching a motor vehicle. In deriving the equation, the sum of the forces brings in the pressure effect acting on the incremental area of the body of fluid. Equating this to the time rate of change of momentum brings in the velocity term.

Bernoulli's equation states that the static plus the dynamic pressure of the air will be constant (P_t) as it approaches the vehicle. Visualizing the vehicle as stationary and the air moving (as in a wind tunnel), the air streams along lines, appropriately called "streamlines." A bundle of streamlines forms a streamtube. The smoke streams used in a wind tunnel allow streamtubes to be visualized as illustrated in Figure 4.1.

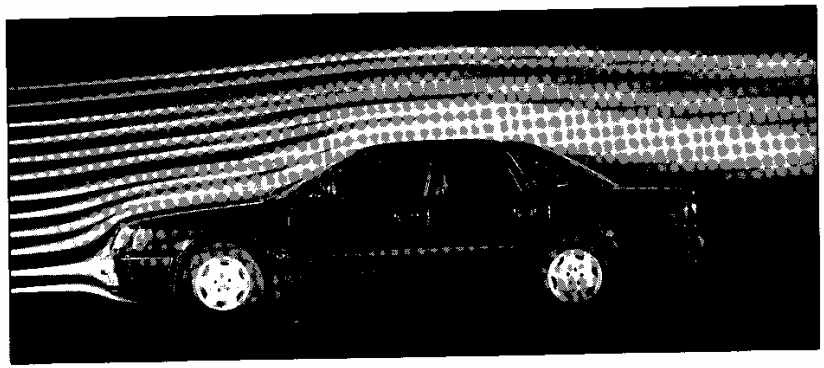

Fig. 4.1 Streamtubes flowing over an aerodynamic body. (Photo courtesy of Audi Division.)

At a distance from the vehicle the static pressure is simply the ambient, or barometric, pressure (P_{atm}). The dynamic pressure is produced by the relative velocity, which is constant for all streamlines approaching the vehicle. Thus the total pressure, P_t, is the same for all streamlines and is equal to $P_s + 1/2\,\rho\,V^2$.

As the flow approaches the vehicle, the streamtubes split, some going above the vehicle, and others below. By inference, one streamline must go straight to the body and stagnate (the one shown impinging on the bumper of the car). At that point the relative velocity has gone to zero. With the velocity term zero, the static pressure observed at that point on the vehicle will be P_t. That is, if a pressure tap is placed on the vehicle at this point, it will record the total pressure.

Consider what must happen to the streamlines flowing above the hood. As they first turn in the upward direction, the curvature is concave upward. At a distance well above the vehicle where the streamlines are still straight, the static pressure must be the same as the ambient. In order for the air stream to be curved upward, the static pressure in that region must be higher than ambient to provide the force necessary to turn the air flow. If the static pressure is higher, then the velocity must decrease in this region in order to obey Bernoulli's Equation.

Conversely, as the flow turns to follow the hood (downward curvature at the lip of the hood) the pressure must go below ambient in order to bend the flow, and the velocity must increase. These points are illustrated in Figure 4.2, showing flow over a cylinder.

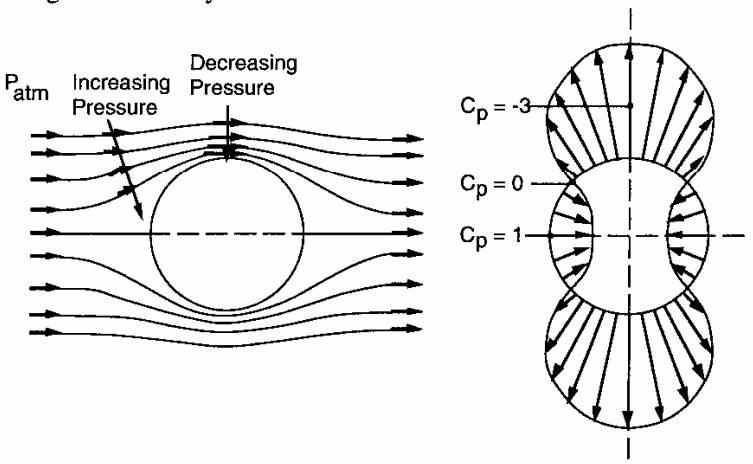

Fig 4.2 Pressure and velocity gradients in the air flow over a body.

Thus Bernoulli's Equation explains how the pressure and velocity must vary in the gross air flow over a car body. In the absence of friction the air would simply flow up over the roof and down the back side of the vehicle, exchanging pressure for velocity as it did at the front. In that case, the pressure forces on the back side of the vehicle would exactly balance those on the front, and there would be no drag produced.

From experience, however, we know that drag is produced. The drag is due in part to friction of the air on the surface of the vehicle, and in part to the way the friction alters the main flow down the back side of the vehicle. Its explanation comes about from understanding the action of boundary layers in the flow over an object. Consider a uniform flow approaching a sharp-edged body as shown in Figure 4.3.

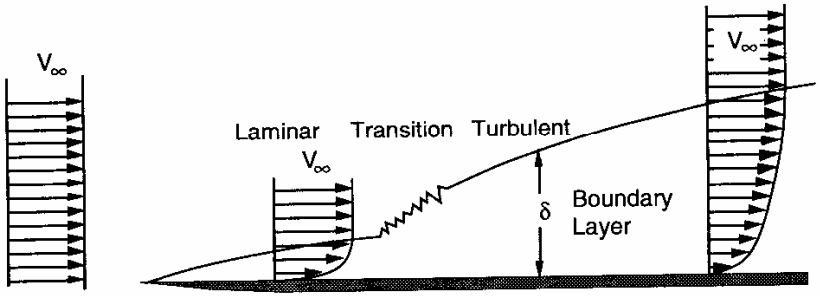

Fig 4.3 Development of a boundary layer.

Approaching the body, all air is traveling at a uniform velocity (and is assumed to be well-behaved, laminar flow). As it flows past the body, the air contacting the surface must drop to zero velocity due to friction on the surface. Thus a velocity profile develops near the surface, and for some distance, δ, the velocity is less than that of the main flow. This region of reduced velocity is known as the "boundary layer." The boundary layer begins with zero thickness and grows with distance along the body. Initially, it too is laminar flow, but will eventually break into turbulent flow.

On the front face of a vehicle body, the boundary layer begins at the point where the stagnation streamline hits the surface. In the boundary layer the velocity is reduced because of friction. The pressure at the stagnation point is the total pressure (static plus dynamic) and decreases back along the surface.

The pressure gradient along the surface thus acts to push the air along the boundary layer, and the growth of the layer is impeded. Pressure decreasing in the direction of flow is thus known as a "favorable pressure gradient," because it inhibits the boundary layer growth.

Unfortunately, as the flow turns again to follow the body, the pressure again increases. The increasing pressure acts to decelerate the flow in the boundary layer, which causes it to grow in thickness. Thus it produces what is known as an "adverse pressure gradient." At some point the flow near the surface may actually be reversed by the action of the pressure as illustrated in Figure 4.4. The point where the flow stops is known as the "separation point." Note that at this point, the main stream is no longer "attached" to the body but is able to break free and continue in a more or less straight line. Because it tries to entrain air from the region behind the body, the pressure in this region drops below the ambient. Vortices form and the flow is very irregular in this region. Under the right conditions, a von-Karman Vortex Street may be formed, which is a periodic shedding of vortices. Their periodic nature can be perceived as aerodynamic buffeting. The vortex action in flow over a cylinder is shown in Figure 4.5.

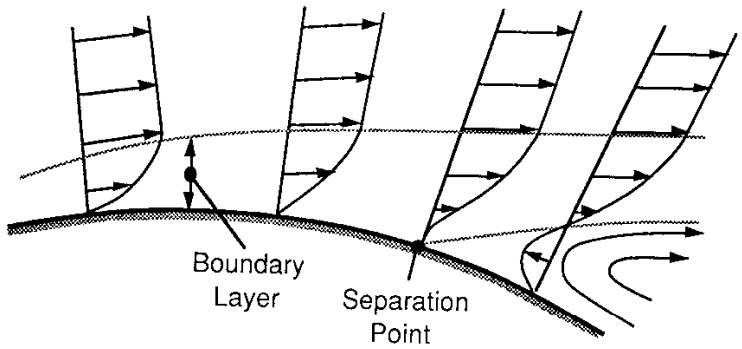

Fig. 4.4 Flow separation in an adverse pressure gradient.

The phenomenon of separation prevents the flow from simply proceeding down the back side of a car. The pressure in the separation region is below that imposed on the front of the vehicle, and the difference in these overall pressure forces is responsible for "form drag." The drag forces arising from the action of viscous friction in the boundary layer on the surface of the car is the "friction drag."

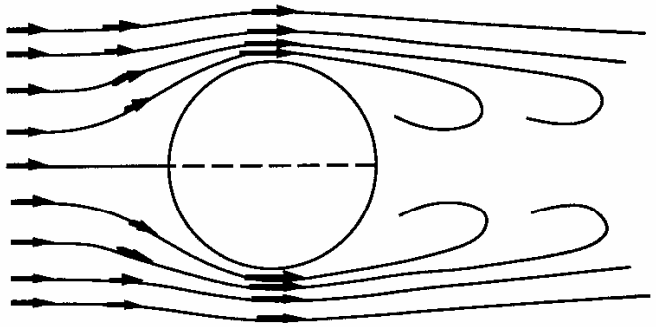

Fig. 4.5 Vortex shedding in flow over a cylindrical body.

Pressure Distribution on a Vehicle

These basic mechanisms account for the static pressure distribution along the body of a car. Figure 4.6 shows experimentally measured pressures [3] plotted perpendicular to the surface. The pressures are indicated as being negative or positive with respect to the ambient pressure measured some distance from the vehicle.

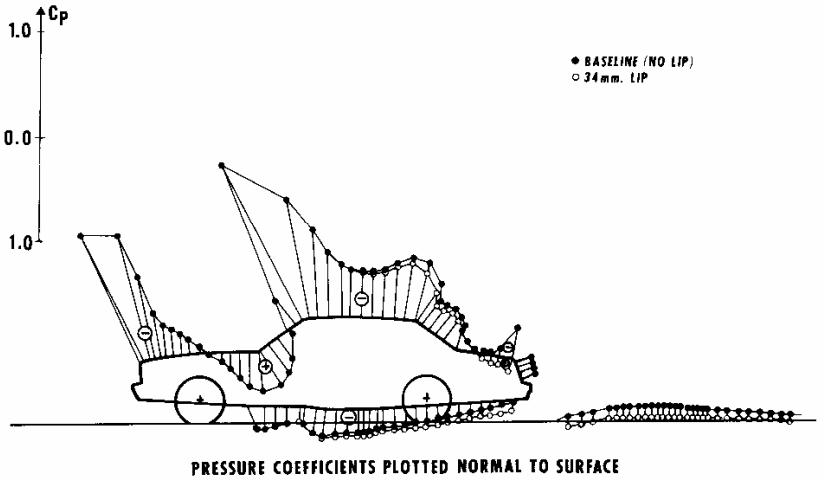

Fig. 4.6 Pressure distribution along the centerline of a car.

Note that a negative pressure is developed at the front edge of the hood as the flow rising over the front of the vehicle attempts to turn and follow horizontally along the hood. The adverse pressure gradient in this region has the potential to stall the boundary layer flow creating drag in this area. In recent years, styling detail in the front hood line has been given high priority to avoid separation on the hood and the drag penalty that results.

Near the base of the windshield and cowl, the flow must be turned upward, thus high pressure is experienced. The high-pressure region is an ideal location for inducting air for climate control systems, or engine intake, and has been used for this purpose in countless vehicles in the past. The high pressures are accompanied by lower velocities in this region, which is an aid to keeping the windshield wipers from being disturbed by aerodynamic forces.

Over the roof line the pressure again goes negative as the air flow tries to follow the roof contour. Evidence of the low pressure in this region is seen in the billowing action of the fabric roof on convertibles. The pressure remains low down over the backlite and on to the trunk because of the continuing curvature. It is in this area that flow separation is most likely. Design of the angles and details of the body contour in this region require critical concern for aerodynamics. Because of the low pressure, the flow along the sides of the car will also attempt to feed air into this region [4] and may add to the potential for separation. The general air flow patterns over the top and sides of a car are shown in Figure 4.7. The flow along the sides is drawn up into the low-pressure region in the rear area, combining with flow over the roof to form vortices trailing off the back of the vehicle.

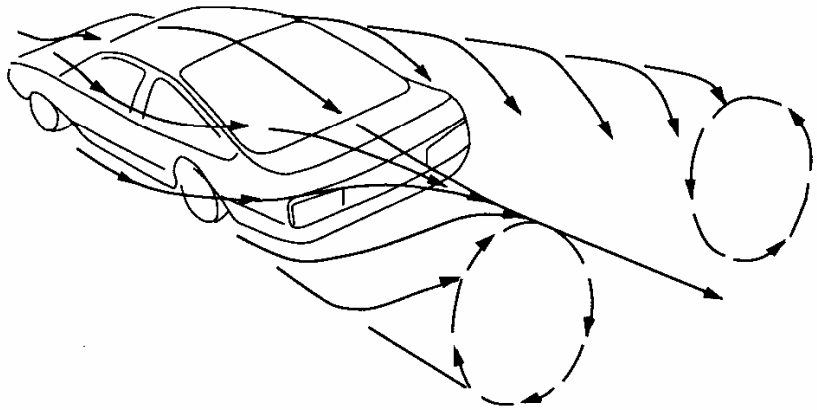

Fig. 4.7 Vortex systems in the wake of a car.

The choice of the backlite angles and deck lid lengths on the back of a car has a direct impact on aerodynamic forces through control of the separation point. Separation must occur at some point, and the smaller the area, generally the lower the drag. Theoretically, the ideal from an aerodynamic viewpoint is a teardrop rear shape, i.e., a conical shape that tapers off to a point with shallow angles of 15 degrees or less. It was recognized as early as the 1930s that because the area toward the point of the cone is quite small, the end of the ideal vehicle can be cut off without much penalty of a large separation area [5, 6, 7]. The blunt rear end shape allows greater head room in the back seat without substantially increasing drag. This characteristic shape has acquired the name "Kamm-back."

While the size of the separation area affects the aerodynamic drag directly, the extent to which the flow is forced to turn down behind the vehicle affects the aerodynamic lift at the rear. Figure 4.8 illustrates the effect on lift and drag for four styles of vehicle [4]. Flow control that minimizes the separation area generally results in more aerodynamic lift at the rear because of the pressure reduction as the flow is pulled downward.

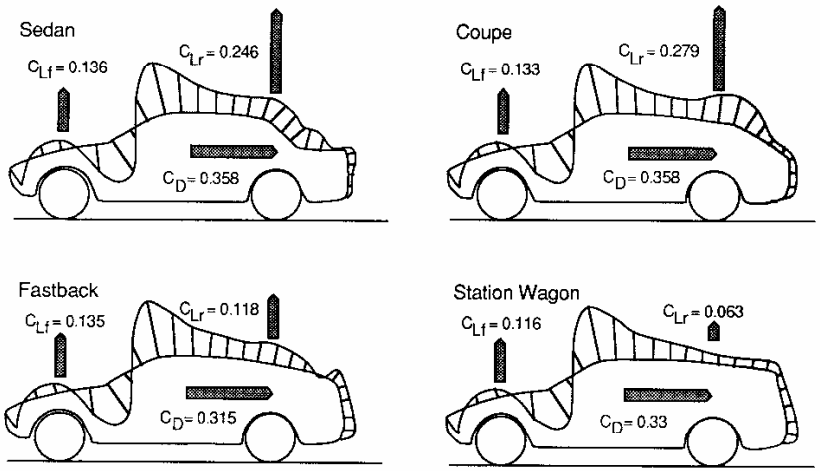

Fig 4.8 Aerodynamic lift and drag forces with different vehicle styles.

Another consideration in aerodynamic design at the rear is the potential for dirt deposition on the backlite and tail lights. The high degree of turbulence in the separation zone entrains moisture and dirt kicked up from the roadway by the tires. If the separation zone includes these items, dirt will be deposited on

these areas and vision will be obstructed. Figure 4.9 illustrates this phenomenon.

Whether separation will occur at the rear edge of the roof line is strongly dependent on the shape at that location and the backlite angle. For the vehicle on the left, the sharp edge at the roof line promotes separation at this point. While a well-defined separation boundary helps minimize aerodynamic buffeting, the inclusion of the backlite in the separation area promotes dirt deposition on the window.

Although the vehicle on the right has a comparable backlite angle, the smooth transition at the rear of the roof and the addition of a modest trunk extension encourages the air stream to follow the vehicle contours down the rear deck. The separation region is well defined by the sharp contours at the end of the deck, helping to stabilize the separation zone and minimize buffeting. Only the tail light region is exposed to road dirt with this design.

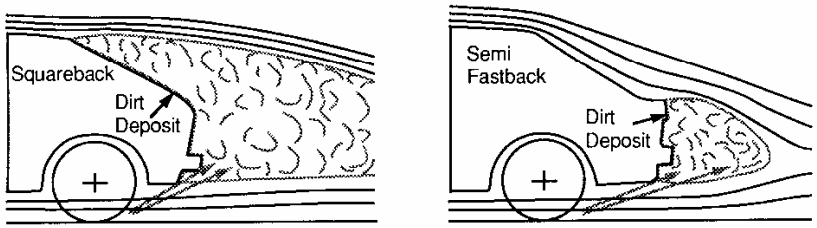

Fig 4.9 Effect of separation point on dirt deposition at the rear.

Aerodynamic Forces

As a result of the air stream interacting with the vehicle, forces and moments are imposed. These may be defined systematically as the three forces and three moments shown in Figure 4.10, acting about the principal axes of the car [8]. The reactions are as follows:

Direction	Force	Moment
Longitudinal (x-axis, positive rearward)	Drag	Rolling moment
Lateral (y-axis, positive to the right)	Sideforce	Pitching moment
Vertical (z-axis, positive upward)	Lift	Yawing moment

The origin for the axis system is defined in SAE J1594 [9]. Inasmuch as the aerodynamic reactions on a vehicle are unrelated to its center of gravity location (and the CG location may not be known in wind tunnel tests), the origin for force measurement is in the ground plane at the mid-wheelbase and mid-track position.

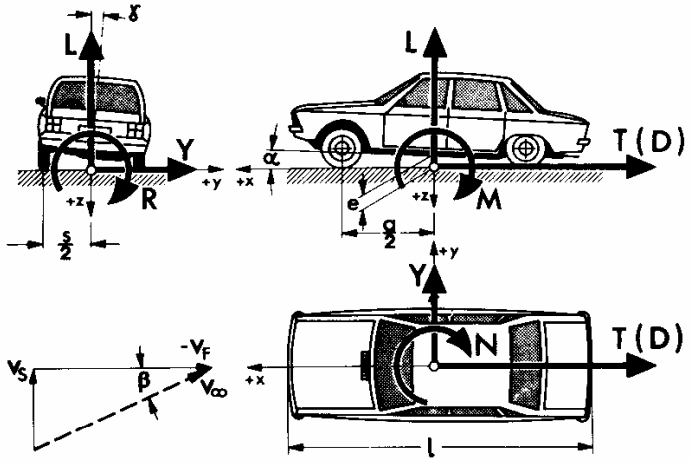

Fig 4.10 Aerodynamic forces and moments acting on a car [14].

Drag Components

Drag is the largest and most important aerodynamic force encountered by passenger cars at normal highway speeds. The overall drag on a vehicle derives from contributions of many sources. Various aids may be used to reduce the effects of specific factors. Figure 4.11 lists the main sources of drag and the potential for drag reductions in these areas estimated for cars in the 1970s.

For the vehicle represented in the figure, approximately 65% (.275/.42) of the drag arises from the body (forebody, afterbody, underbody and skin friction). The major contributor is the afterbody because of the drag produced by the separation zone at the rear. It is in this area that the maximum potential for drag reduction is possible. Figure 4.12 shows the influence of rear end inclination angle on the drag for various lengths of rear extension (beyond the rear edge of the roof line) [10]. Slope angles up to 15 degrees consistently reduce drag. As the angles increase, the drag again increases because of flow

separation. (In practice, higher drop angles have been achieved without separation.)

DRAG COEFFICIENT COMPONENT	TYPICAL VALUE
Forebody	0.05
Afterbody	0.14
Underbody	0.06
Skin Friction	0.025
Total Body Drag	0.275
Wheels and wheel wells	0.09
Drip rails	0.01
Window recesses	0.01
External mirrors	0.01
Total Protuberance Drag	0.12
Cooling system	0.025
Total Internal Drag	0.025
Overall Total Drag	0.42[1]
VEHICLE OF THE 1980s	
Cars	0.30 - 0.35
Vans	0.33 - 0.35
Pickup trucks	0.42 - 0.46

[1] Based on cars of 1970s vintage.

Fig. 4.11 Main sources of drag on a passenger car.

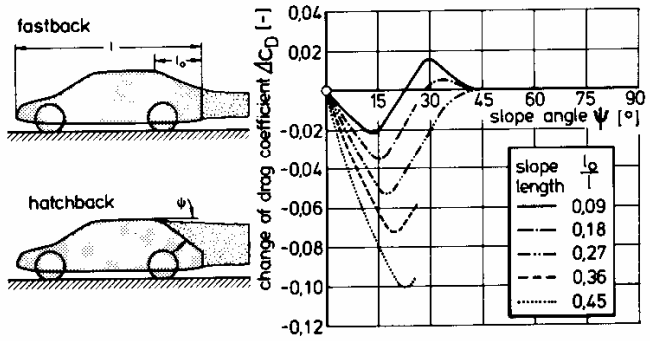

Fig 4.12 Influence of rear end inclination on drag.

Forebody drag is influenced by design of the front end and windshield angle. Generally the "roundness" of the front end establishes the area over which the dynamic pressure can act to induce drag. Figure 4.13 shows the influence of the height of the front edge of the vehicle [10]. The location of this point determines the location of the streamline flowing to the stagnation point. This streamline is important as it establishes the separation of flow above and below the body. Minimum drag is obtained when the stagnation point is kept low on the frontal profile of the vehicle. A well-rounded shape, in contrast to the crisp lines traditionally given to the frontal/grill treatment of passenger cars, is equally important to aerodynamics. A rounded low hood line can yield reductions of 5 to 15% in the overall drag coefficient [11].

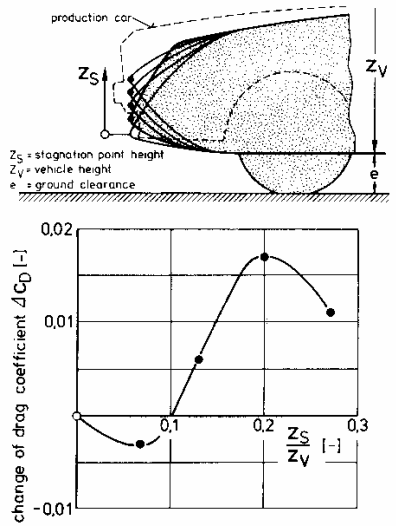

Fig 4.13 Influence of front end design on drag.

The windshield establishes the flow direction as it approaches the horizontal roof. Thus its angle has a direct influence on drag, particularly on trucks. Shallow angles reduce drag, but complicate vehicle design by allowing increased solar heating loads and placing more critical demands on the manufacturer of the windshield to minimize distortion at shallow angles. Figure 4.14 shows the change in drag as the windshield angle is increased from the nominal angle of 28 degrees [10]. With a steep angle, the air velocity

approaching the windshield is reduced by the high pressure in that region. With a shallow angle, the wind speed will be higher, adding to the aerodynamic loads on the windshield wipers.

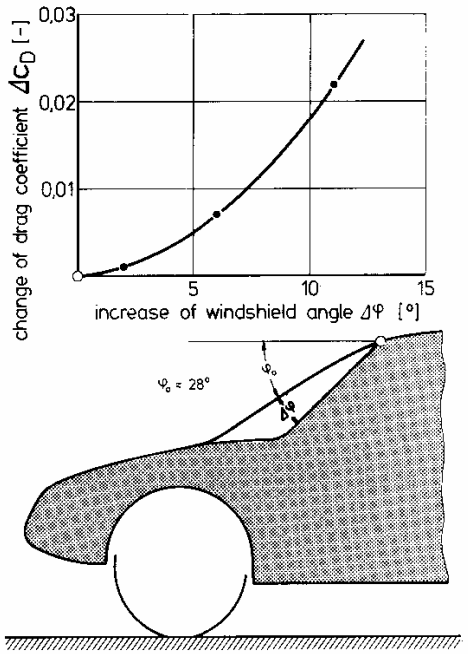

Fig. 4.14 Influence of windshield angle on drag.

The underbody is a critical area generating body drag. Suspensions, exhaust systems and other protruding components on the underbody are responsible for the drag. The air flow in this area is a shear plane controlled by zero air speed on the road surface, and induced flow by drag of the underbody components. The recognized fix for minimizing underbody drag is the use of a smooth underbody panel.

Protuberances from the body represent a second area where careful design can reduce drag. The wheels and wheel wells are a major contributor in this class. Significant drag develops at the wheels because of the turbulent, recirculating flow in the cavities. Figure 4.15 illustrates the complex flow

patterns that occur around a wheel [13]. The sharp edges of the wheel cutout provide opportunities to induce flow in the horizontal plane, while the rotating wheel tends to induce circulation in the vertical plane. These effects allow the wheel to influence more flow than simply that which is seen because of its frontal area presented to the flow. The obvious improvement is aerodynamic shielding of the wheels and wheel well areas. While this is possible to some extent on rear wheels, steer rotation on the front wheels complicates the use of such treatment at the front. Experimental research has shown that decreasing the clearance between the underside and the ground and minimizing the wheel cavity decreases the total aerodynamic drag contribution from the wheel [12].

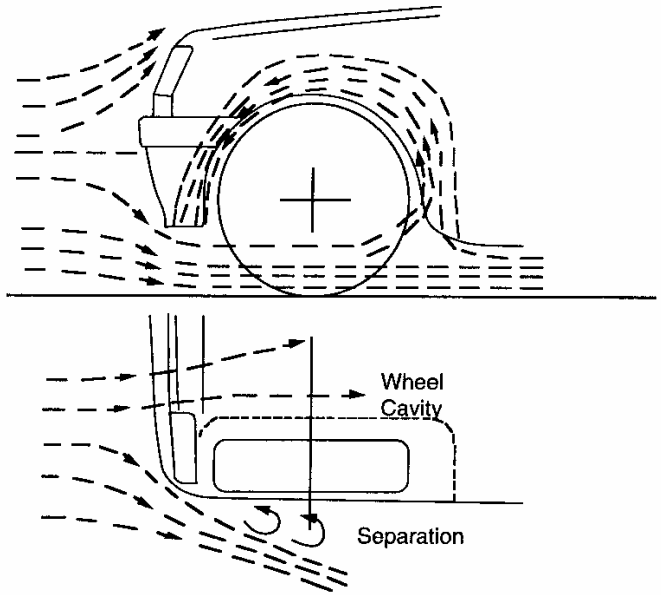

Fig 4.15 Air flow recirculation in a wheel well.

The cooling system is the last major contributor to drag. Air flow passing through the radiator impacts on the engine and the firewall, exerting its dynamic pressure as drag on the vehicle. The air flow pattern inside a typical engine compartment may be very chaotic due to the lack of aerodynamic treatment in this area. Figure 4.16 illustrates this situation [12]. With no attention to the need for air flow management, the air entering through the radiator dissipates much of its forward momentum against the vehicle compo-

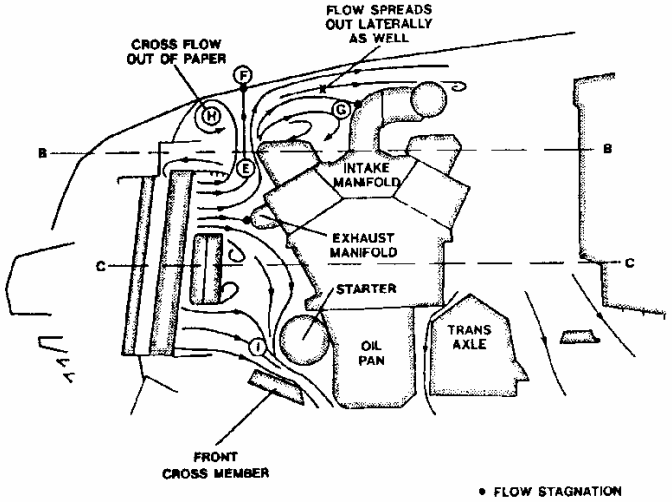

Fig 4.16 Air flow pattern inside a typical engine compartment. (Source: Williams, J., Ohler, W., Hackett, J., and Hammar, L., "Water Flow Simulation of Automotive Underhood Air Flow Phenomena," SAE Paper No. 910307, SP-855, 1991, 31 p.)

nents in the engine compartment before spilling out through the underside openings. The momentum exchange translates directly into increased drag.

Flow management in the cooling system can affect the drag coefficient by as much as 0.025 [10]. The drag contribution from this source is normally taken to be the difference in drag measured with the cooling system inlets open and covered. As seen in Figure 4.17, careful design to direct the flow (allowing it to maintain its velocity so that the static pressure remains low) can reduce the drag produced. Although these various arrangements may not be feasible within the styling theme of a given car, the potential for aerodynamic improvements is evident in the drag reductions shown. In order to reduce drag on modern cars, cooling inlet size is held to the practical minimum.

Aerodynamic Aids

Bumper Spoilers

Front bumper spoilers are aerodynamic surfaces extending downward from the bumper to block and redirect the shear flow that impacts on the underbody components. While the spoiler contributes pressure drag, at least